ESCRT-dependent membrane repair negatively regulates pyroptosis downstream of GSDMD activation

One sentence summary:

ESCRT restricts membrane damage by GSDMD.

Authors:

Sebastian Rühl[1], Kateryna Shkarina[2, ‡], Benjamin Demarco[2, ‡], Rosalie Heilig[2, ‡], José Carlos Santos[2, ‡] and Petr Broz[1, 2, *]

Affiliations:

[1] Focal Area Infection Biology, Biozentrum, University of Basel, Klingelbergstrasse 50/70, 4056 Basel, Switzerland

[2] Department of Biochemistry, University of Lausanne, Chemin des Boveresses 155, 1066 Epalinges, Switzerland

* corresponding author: petr.broz@unil.ch

‡ these authors contributed equally

Abstract

Pyroptosis is a lytic form of cell death that is induced by inflammatory caspases upon activation of the canonical or non-canonical inflammasome pathways. These caspases cleave gasdermin D (GSDMD) thereby generating an N-terminal GSDMD fragment that executes pyroptosis by forming membrane pores. Here, we find that calcium influx through GSDMD pores serves a signal for cells to initiate membrane repair by recruiting the ESCRT machinery to damaged membrane areas, such as the plasma membrane. Inhibition of the ESCRT-III machinery strongly enhances pyroptosis and IL-1β release in both human and murine cells after canonical or non-canonical inflammasome activation. These results not only attribute an anti-inflammatory role to membrane repair by the ESCRT-III system, but also provide insight in general cellular survival mechanisms during pyroptosis.

Main text

Gasdermin D (GSDMD) is a pore-forming protein that causes pyroptosis, a necrotic cell death that is initiated after inflammasome activation (*1*–*3*). Detection of pathogen- or host-derived danger signals by inflammasomes triggers the activation of inflammatory caspases, caspase-1 and -11 in mice or caspase-1 and -4 in humans, which cleave GSDMD to release autoinhibition on its N-terminal domain ($GSDMD^{NT}$) (*1*, *2*). The $GSDMD^{NT}$ targets the plasma membrane and organelles, where it forms large pores to execute pyroptosis (*4*–*7*). Damage to the plasma membrane does not necessarily result in cell death, since it has been observed that the influx of Ca^{2+} ions from the extracellular milieu triggers repair programs involving either the endocytosis of damaged membrane or its shedding in form of ectosomes (*8*–*11*). The later mechanism relies on components of endosomal sorting complexes required for transport (ESCRT)-0, -III, and associated factors that control ESCRT recruitment and disassembly, and

has been specifically implicated in the restoration of plasma membrane integrity during necroptosis (*12*) or upon chemical or laser-induced damage (*10*, *11*).

To investigate if cells repair membranes damaged by GSDMD pores, we imaged the disruption of the electrochemical gradient (Ca^{2+} dye Fluo-8) and loss of membrane integrity (Propidium iodide, PI) in mouse bone marrow-derived macrophages (BMDMs) that were left untreated or transfected with LPS to activate caspase-11. Within 2 hours, up to 50% of LPS-transfected wildtype (WT) BMDMs underwent pyroptosis as indicated by strong PI signal (PI^{hi}) (**Fig. S1A**). A marked spike of Fluo-8 signal preceded the PI^{hi} signal, indicating a loss of membrane integrity and Ca^{2+} influx (**Fig. 1A-B, S1B-D, Movie 1-2**). By contrast, Fluo-8 or PI signals did not change in *Casp11*$^{-/-}$ or *Gsdmd*$^{-/-}$ BMDMs (**Fig. 1B, S1C-D, Movie 1-2**). Unexpectedly, we found that Ca^{2+}-influx-negative WT BMDMs that maintained the electrochemical gradient gradually acquired a low-level PI staining (**Fig. 1C**). This PI^{lo} signal only reached 1/10 of the PI^{hi} signal observed in WT BMDMs that had lost membrane integrity upon LPS transfection. Furthermore, neither unstimulated WT BMDMs (**Fig. 1A**) nor LPS-transfected *Casp11*$^{-/-}$ or *Gsdmd*$^{-/-}$ cells showed such a PI^{lo} signal (**Fig. 1C**). This confirmed that low-level PI influx was caused by GSDMD pores, and given the absence of a Fluo-8 signal peak, implied that PI^{lo} cells had repaired their plasma membrane to prevent lysis.

Next, we used the Ca^{2+} chelators BAPTA-AM or EDTA to block membrane repair as done previously (*10*, *11*). Ca^{2+} chelators increased the levels of cell lysis and lactate dehydrogenase (LDH) release from WT BMDMs after LPS transfection in a dose dependent manner (**Fig. 1D, S1A, S2**). Importantly, Ca^{2+} chelation was not cytotoxic (**Fig. 1D, S2A**) and did not enhance LPS transfection or caspase-11 activation as assessed by immunoblotting for $GSDMD^{NT}$ (**Fig. 1E, S3A**). BAPTA-AM also increased caspase-4-dependent pyroptosis without significantly altering GSDMD processing in HeLa cells infected with *ΔsifA Salmonella typhimurium* (**Fig.**

1F-G, S3B)(*13*). In summary, Ca^{2+} chelation enhanced pyroptosis in human and mouse cells, potentially by preventing the initiation of plasma membrane repair.

ESCRT proteins target membranes during membrane repair to form a punctate pattern (*10*, *12*). Consistently, CHMP4 puncta were observed in HeLa cells, expressing CHMP4-GFP from its endogenous promoter (*14*), after *S. typhimurium* infection, $GSDMD^{NT}$ expression, or perforin treatment (control), but not in untreated cells (**Fig. S4, Movie 3**). Moreover, Ca^{2+} chelation significantly reduced the number of CHMP4-GFP-puncta-positive cells (**Fig. 2A**), indicating that ESCRT assembly requires Ca^{2+} influx via GSDMD pores. Next, we transfected CHMP4-mCherry or CHMP4-GFP into HEK293T cells stably expressing caspase-1 fused with a modified FKBP domain (DmrB-Casp-1). Following dimerization and activation of DmrB-Casp-1 with B/B homodimerizer, cells underwent pyroptosis as demonstrated by morphological changes and plasma membrane Annexin-V staining (**Fig. 2B-C, movie 4-6**). CHMP4 re-localized to a punctate pattern in DmrB-Casp-1-transgenic HEK293Ts expressing either high (**Fig. 2B-C, S5A-C arrows**) or low levels of CHMP4 (**Fig. S5B**), and similar CHMP4 puncta were detected after activation of DmrB-Casp-11 (**Fig. S6A**). Although many CHMP4 puncta clearly localized to the plasma membrane (**Fig. 2B-C, S4-6, movie 6**), puncta also formed in the cytoplasm, presumably on intracellular organelles. During necroptosis, the ESCRT machinery promotes the formation of Annexin-V^+ plasma membrane vesicles, which were proposed to remove damaged plasma membrane areas (*12*). Similar Annexin-V positive vesicles were detected budding-off from HEK293T cells after activation of DmrB-Casp-1 (**Fig. 2C-D, S5D, Movie 5**) or DmrB-Casp-11 (**Fig. S6B**). Importantly, these vesicles showed clear CHMP4 puncta at their neck (**Fig. 2C, S5D, S6B**), and when $GSDMD\text{-}GFP^{internal}$ (**Fig. S7A**) was co-expressed, it localized close to CHMP4-mCherry puncta on the cell periphery (**Fig. S7B**) and on the membrane of Annexin-V^+ vesicles (**Fig. 2D, S7C**), suggesting that ESCRT-induced ectosomes remove GSDMD pores from the plasma membrane.

Next, we examined the impact of ESCRT-III inactivation on inflammasome effector functions. We transiently expressed either WT or dominant-negative CHMP3 or VPS4A in immortalized mouse BMDMs (iBMDMs) or HeLa cells (**Fig. S8A-C**), since prolonged ESCRT depletion is cytotoxic (*10*, *12*). Expression of dominant-negative $VPS4A^{E228Q}$ or $CHMP3^{1-179}$ inhibited ESCRT disassembly as verified by a punctate pattern (**Fig. S8D**), and reduced cell viability after 20-24 hours of expression (**Fig. S8E**), prompting us to restrict our experiments to a maximum 15 hours post-induction with doxycycline. Expression of $VPS4A^{E228Q}$ in WT iBMDMs resulted on 2-to-4-fold higher cell death levels after LPS transfection compared to $VPS4A^{WT}$-expressing controls (**Fig. 3A-B, S9, Movies 7-8**) and decreased recovery after LPS transfection (**Fig. S10**). ESCRT inactivation also strongly enhanced IL-1β release after LPS transfection (**Fig. 3C**), but importantly neither enhanced LDH or cytokine release from untreated, *Casp11*$^{-/-}$ or *Gsdmd*$^{-/-}$ cells (**Fig. S11**). IL-1β release after non-canonical inflammasome activation depends on GSDMD-induced K^+ efflux and subsequent activation of the NLRP3-caspase-1 pathway (*15*, *16*). Since LPS-transfected WT iBMDMs expressing $VPS4A^{E228Q}$ had higher levels of processed, activated caspase-1 and released more mature IL-1β than $VPS4A^{WT}$-expressing control cells (**Fig. 3C-D**), we speculated that it is due to enhanced K^+ efflux through increased GSDMD pore formation. Consistently, and in agreement with previous reports (*15*), cytokine release but not cell death was attenuated by treatment with the NLRP3 inhibitor MCC950 or high extracellular K^+ (**Fig. 3E, S12A).**

We next assayed GSDMD processing and found that $GSDMD^{NT}$ levels were slightly enhanced in $VPS4A^{E228Q}$ transgenic iBMDMs compared to $VPS4A^{WT}$ transgenic iBMDMs at high LPS concentrations (**Fig. 3F**). We postulated that enhanced GSDMD processing was caused by enhanced NLRP3 inflammasome activation (**Fig. 3E, S12A**), and was thus caspase-1-dependent. Indeed, GSDMD processing was unchanged between $VPS4A^{E228Q}$ and $VPS4A^{WT}$-

expressing iBMDMs in the presence of MCC950 (**Fig. 3F, S12B**), confirming that ESCRT negatively regulates pyroptosis downstream of caspase-11 activation and GSDMD processing.

To study the role of ESCRT-associated proteins, we knocked-down expression of ESCRT-I/III proteins, and two proteins, ALG2 and ALIX, implicated in Ca^{2+}-dependent recruitment of ESCRTs (*8*). As spontaneous necroptosis occurs upon ESCRT depletion (*12*), we did all knockdowns in *Ripk3*$^{-/-}$ iBMDMs (*12*), which remained viable despite successful protein depletion (**Fig. S13A-E)**. Knockdown of CHMP3, VPS4A and VPS4B significantly enhanced pyroptosis and IL-1β release in *Ripk3*$^{-/-}$ iBMDMs transfected with LPS (**Fig. 3G**). By contrast, single- or double-knockdowns of ALIX and ALG-2 had no impact on pyroptosis (**Fig. 3G**). ALG2 and ALIX might act redundantly with TSG101 (*17*), but simultaneous depletion was not possible due to the cytotoxicity of TSG101 depletion in BMDMs (**Fig. S13F**).

ESCRT inactivation also enhanced pyroptosis in human cells infected with Δ*sifA S. typhimurium* (**Fig. S14A-D**). Here ESCRTs appeared to have an additional function upstream of inflammasomes, since ESCRT inactivation resulted in higher levels of ruptured, Galectin-3^{+} *Salmonella*-containing vacuoles (**Fig. S15A-C**), despite equal levels of bacterial invasion (**Fig. S14E-F**). This implied that ESCRTs could repair damaged vacuoles/endosomes as published recently (*17*) and thereby control bacterial escape into the cytosol. However, the elevated levels of cytosolic bacteria in ESCRT-depleted cells had only a negligible impact on GSDMD processing at the timepoints examined (**Fig. S15D-F**).

We next asked if ESCRTs also regulate cell death after canonical inflammasome activation. Ca^{2+} chelation significantly enhanced pyroptosis after DNA transfection of BMDMs (**Fig. S16A-B**), without changing caspase-1 processing (**Fig. S16C-D**). Furthermore, ESCRT depletion significantly enhanced cell death and IL-1β release in iBMDMs following NLRC4 activation with log-phase *S. typhimurium*, but did not enhance ASC speck formation or processing of caspase-1 or GSDMD (**Fig. 4A-B, S17**), indicating that ESCRTs restrict

pyroptosis downstream of GSDMD. To further exclude any effects of ESCRT depletion on the upstream signals that control caspase-1 activation, we used DmrB-Casp-1-transgenic HEK293T cells. Activation of DmrB-Casp-1 caused pyroptosis with faster kinetics in cells expressing dominant-negative $VPS4A^{E228Q}$ or $CHMP3^{1-179}$ compared to cells expressing the WT proteins, in particular if DmrB-Casp-1 activity was limited by adding an inhibitory washout compound (**Fig. 4C, S18A**). B/B homodimerizer enhanced pyroptosis in ESCRT-deficient compared to ESCRT-proficient cells across a variety of concentrations (**Fig 4D**, **S18B**). Importantly, ESCRT inactivation did not affect GSDMD processing (**Fig 4E, S18C**) and only enhanced pyroptosis in DmrB-Casp-1-transgenic HEK293Ts when GSDMD was co-expressed (**Fig. S18D-E**). Finally, ESCRT-inactivation also enhanced IL-1β release, as shown using pro-IL-1β-transgenic HEK293T cells (**Fig 4F, S18F**).

Thus, in a variety of cell lines and systems, the ESCRT machinery dampens GSDMD pore-mediated cell death and negatively regulates IL-1β secretion following canonical and non-canonical inflammasome activation. We propose that ESCRTs play a central role in removing GSDMD pores from the plasma membrane in the form of ectosomes and that membrane repair could allow cells to restrict pyroptosis while permitting limited GSDMD-dependent cytokine release (*18*, *19*). Our results place ESCRTs downstream of caspase activation and GSDMD processing, but do not exclude that ESCRTs also control the activation of inflammasomes, for example by repairing damaged bacteria-containing vacuoles and thus restricting cytosolic access of bacteria-derived ligands. Further experiments are needed to assess this aspect of ESCRTs and to determine if ESCRT-induced vesicles transport cytokines and danger signals.

References and Notes

1. N. Kayagaki *et al.*, Caspase-11 cleaves gasdermin D for non-canonical inflammasome signalling. *Nature*. **526**, 666–71 (2015).

2. J. Shi *et al.*, Cleavage of GSDMD by inflammatory caspases determines pyroptotic cell death. *Nature*. **526**, 660–5 (2015).

3. P. Broz, V. M. Dixit, Inflammasomes: mechanism of assembly, regulation and signalling. *Nat Rev Immunol*. **16**, 407–20 (2016).

4. L. Sborgi *et al.*, GSDMD membrane pore formation constitutes the mechanism of pyroptotic cell death. *EMBO J*. **35**, 1766–78 (2016).

5. R. A. Aglietti *et al.*, GsdmD p30 elicited by caspase-11 during pyroptosis forms pores in membranes. *Proc. Natl. Acad. Sci. U.S.A*. **113**, 7858–7863 (2016).

6. J. Ding *et al.*, Pore-forming activity and structural autoinhibition of the gasdermin family. *Nature*. **535**, 111–6 (2016).

7. X. Liu *et al.*, Inflammasome-activated gasdermin D causes pyroptosis by forming membrane pores. *Nature*. **535**, 153–8 (2016).

8. N. W. Andrews, P. E. Almeida, M. Corrotte, Damage control: cellular mechanisms of plasma membrane repair. *Trends Cell Biol*. **24**, 734–42 (2014).

9. C. Tam *et al.*, Exocytosis of acid sphingomyelinase by wounded cells promotes endocytosis and plasma membrane repair. *J Cell Biol*. **189**, 1027–38 (2010).

10. A. J. Jimenez *et al.*, ESCRT machinery is required for plasma membrane repair. *Science*. **343**, 1247136 (2014).

11. L. L. Scheffer *et al.*, Mechanism of Ca(2)(+)-triggered ESCRT assembly and regulation of cell membrane repair. *Nat Commun*. **5**, 5646 (2014).

12. Y. N. Gong *et al.*, ESCRT-III Acts Downstream of MLKL to Regulate Necroptotic Cell Death and Its Consequences. *Cell*. **169**, 286-300 e16 (2017).

13. J. Shi *et al.*, Inflammatory caspases are innate immune receptors for intracellular LPS. *Nature*. **514**, 187–192 (2014).

14. I. Poser *et al.*, BAC TransgeneOmics: a high-throughput method for exploration of protein function in mammals. *Nat Methods*. **5**, 409–15 (2008).

15. N. Kayagaki *et al.*, Non-canonical inflammasome activation targets caspase-11. *Nature*. **479**, 117–21 (2011).

16. S. Rühl, P. Broz, Caspase-11 activates a canonical NLRP3 inflammasome by promoting K(+) efflux. *Eur. J. Immunol.* **45**, 2927–2936 (2015).

17. M. L. Skowyra, P. H. Schlesinger, T. V. Naismith, P. I. Hanson, Triggered recruitment of ESCRT machinery promotes endolysosomal repair. *Science*. **360** (2018), doi:10.1126/science.aar5078.

18. R. Heilig *et al.*, The Gasdermin-D pore acts as a conduit for IL-1β secretion in mice. *Eur. J. Immunol.* **48**, 584–592 (2018).

19. C. L. Evavold *et al.*, The Pore-Forming Protein Gasdermin D Regulates Interleukin-1 Secretion from Living Macrophages. *Immunity*. **48**, 35-44.e6 (2018).

Author Contributions

S.R. and P.B. designed the study. S.R., K.S., B.D., R.H., J.C.S. and P.B. performed experiments, analyzed data, and wrote the manuscript.

Acknowledgments

We thank Prof. A. Hyman (MPI-CBG, Dresden, Germany) for CHMP4-GFP HeLa cells, Prof. A. Oberst (University of Washington, Seattle, USA) for DmrB-caspase-1, J. Pieters (Biozentrum, Basel) for support and discussions and C. Ramon-Barros for technical assistance. Microscopy analysis was performed at the Biozentrum and UNIL Imaging Core Facilities. This work was supported by grants from the Swiss National Science Foundation (310030_175576) and the ERC (ERC-2017-CoG – 770988 – InflamCellDeath) to P.B. and a Werner Siemens Fellowship (Fellowships for Excellence, University of Basel) to S.R.. The authors declare no competing financial interests. All data are available in the article or in the supplementary materials. Cell lines and plasmids are shared upon request. The authors apologize to investigators whose contributions were not cited extensively because of space limitations.

Supplementary Materials

Material and Methods

Fig. S1-S18

Movies S1-S8

Figure legends

Figure 1. GSDMD-induced calcium flux negatively regulates pyroptosis

A-B. Fluo-8 (Ca^{2+} indicator) and PI signals in unstimulated or LPS-transfected wildtype and *Gsdmd*$^{-/-}$ BMDMs. Graphs show average data from n=22, 22, 28, and 30 cells. **C**. Acquisition of PI^{lo} signal in Ca^{2+} influx-negative wildtype, *Casp11*$^{-/-}$ and *Gsdmd*$^{-/-}$ BMDMs treated as in A. Graphs show average data from n=29, 29, and 26 cells. **D**. LDH release from BAPTA-AM-treated BMDMs mock- or LPS-transfected for 2 hours. **E.** GSDMD processing in HA-GSDMD-transgenic iBMDMs 2 hours post LPS transfection. **F-G.** LDH release and GSDMD processing in untreated or BAPTA-AM-treated HeLa cells infected with Δ*sifA S. typhimurium* for 5 hours. Graphs (**C**, **E**) show mean ± SD. ** P <0.01; **** P<0.0001; ns, not significant; Student's *t*-test. Results are representative of at least three independent experiments.

Figure 2. The ESCRT machinery translocates to the plasma membrane during pyroptosis

A. Fixed-cell microscopy images and CHMP4-GFP puncta quantification of CHMP4-GFP/Dox-inducible $GSDMD^{NT}$ double-transgenic HeLa cells treated with 1 μg/ml of Dox for 4.5 hours. **B-C.** Time-lapsed confocal images of either (B) CHMP4-mCherry-expressing or (C) CHMP4-GFP-expressing DmrB-Casp-1-transgenic HEK293T cells stained with Annexin-V as membrane marker. Insets show CHMP4 localizing to plasma membrane or neck of budding vesicles. **D.** Close-up of Annexin-V^+ vesicle released from CHMP4-mCherry- and $GSDMD\text{-}GFP^{internal}$-expressing DmrB-Casp-1-transgenic HEK293T cells after 1-hour homodimerizer treatment. Graphs show mean ± SD.* P <0.05; ** P<0.01; Student's *t*-test. Results are representative of at least three independent experiments. Arrowheads indicate CHMP4 puncta. Scale bars are 5 (A), 10 (B- C), and 1 μm (D).

Figure 3 ESCRT inactivation enhances non-canonical inflammasome-induced pyroptosis

A-D. PI staining, LDH release, IL-1β release and caspase-1 processing from VPS4A^{WT}- or VPS4A^{E228Q}-transgenic iBMDMs 2 hours after LPS transfection. **E-F.** LDH release, IL-1β release, and GSDMD processing from VPS4A^{WT}- or VPS4A^{E228Q}-transgenic iBMDMs 2 hours post LPS transfection in the presence or absence of 2.5 μM MCC950. **G.** LDH and IL-1β release 4 hours post LPS transfection from *Ripk3*$^{-/-}$ iBMDMs treated with the respective siRNA. Graphs show mean ± SD. ***P* <0.01; ****P*<0.001, *****P*<0.0001; ns, not significant; Student's *t*-test. Results are representative of at least three independent experiments. VPS4A$^{WT/E228Q}$ expression in A-F was induced with 0.5 μg/ml of Dox for 6 hours.

Figure 4. ESCRT negatively regulates pyroptosis and cytokines release downstream of caspase-1

A-B. LDH release, IL-1β release, processing of caspase-1 and GSDMD from VPS4A$^{WT/E228Q}$-transgenic iBMDMs infected with log-phase *S. typhimurium* for 1 hour. **C.** Time course of PI staining in DmrB-Casp1-transgenic HEK293T cells expressing FLAG-hGSDMD-V5 and Dox-inducible VPS4A or CHMP3 constructs. Cells were treated with 25 nM B/B homodimerizer (B/B HD) at t=0 and 50-fold excess washout compound at t=30 minutes. **D.** LDH release at t=120 minutes from DmrB-Casp1-transgenic HEK293T cells treated as in C, except for varying B/B HD concentrations. Immunoblots show equal expression levels of VPS4A proteins. **E.** GSDMD processing at t=60 minutes of DmrB-Casp1-transgenic HEK293T cells treated as in C, except for 50 nM B/B HD. **F.** LDH and IL-1β release at t=90 minutes from DmrB-Casp1- and pro-IL-1β-double transgenic HEK293T expressing FLAG-hGSDMD-V5 and Dox-inducible VPS4A constructs. Cells were treated with B/B HD at t=0 and 50-fold excess washout compound at t=30 minutes. Graphs show mean ± SD. **P*<0.05; ***P* <0.01; ****P*<0.001, *****P*<0.0001; Student's *t*-test (A, D, F) or two-way ANOVA (C).

Results are representative of at least three independent experiments. Protein expression was induced for 6 hours (0.5 μg/ml of Dox, A-B) or 16 hours (1 μg/ml of Dox, C-F).

aar7670 Figure 1

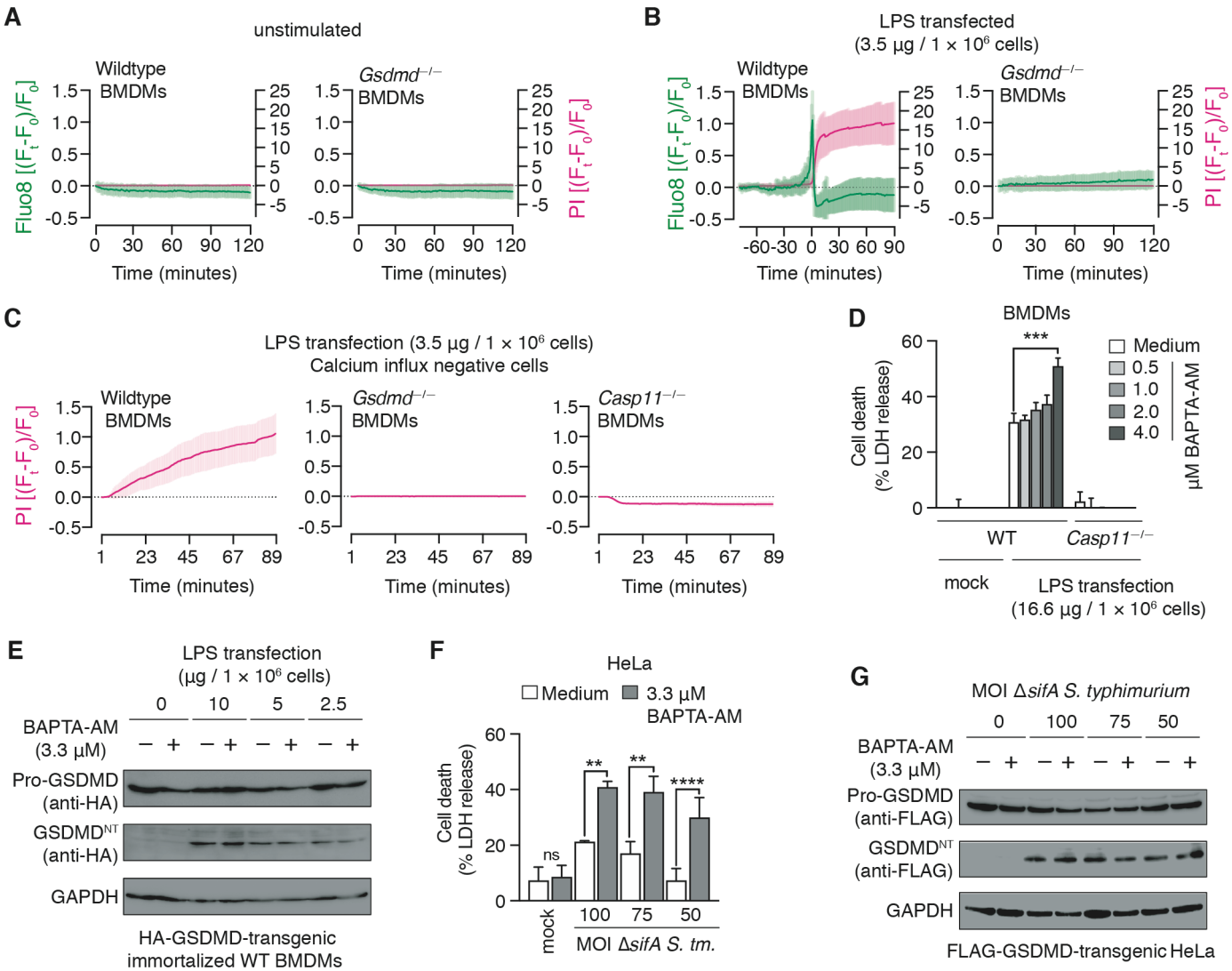

aar7670 Figure 2

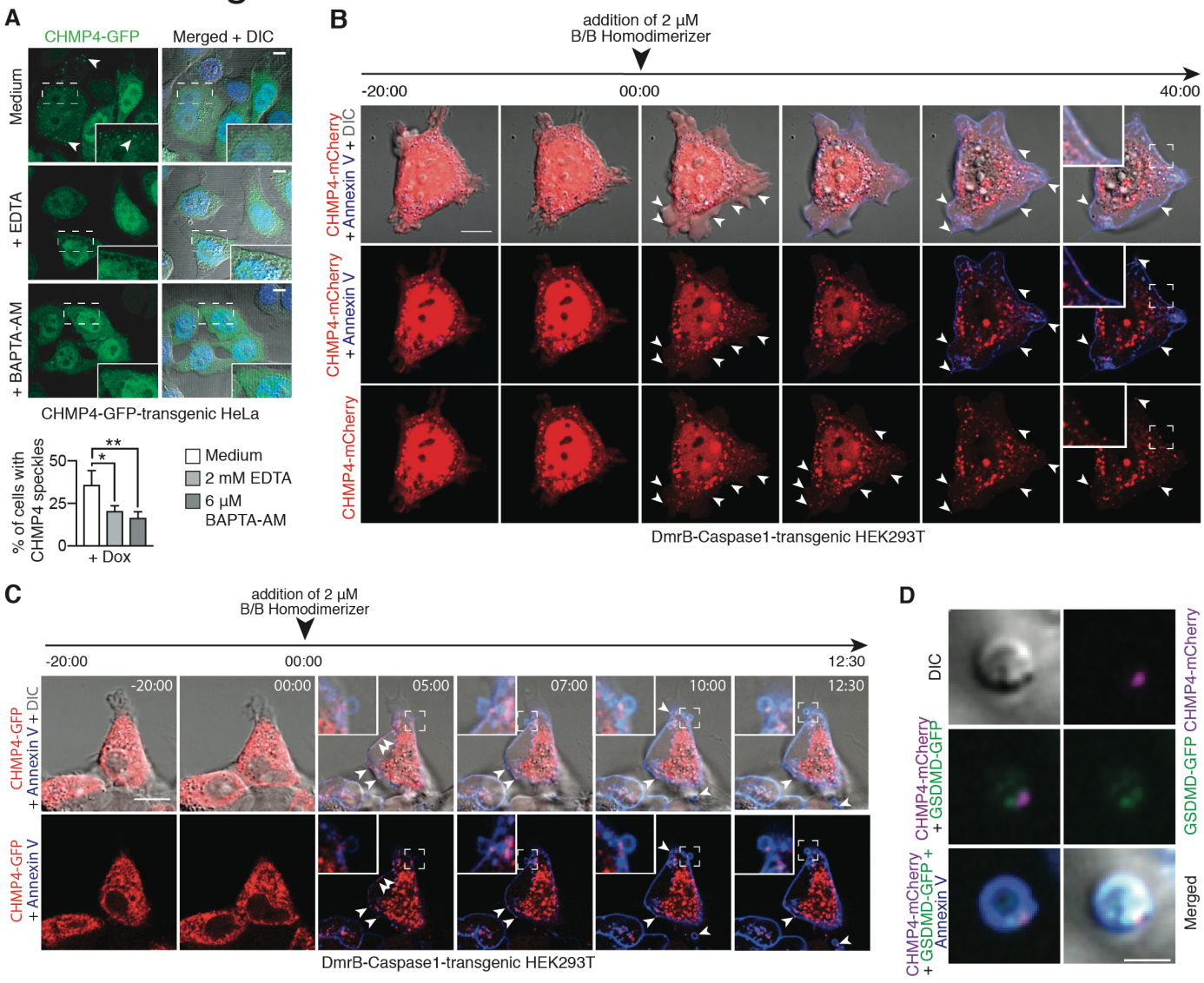

aar7670 Figure 3

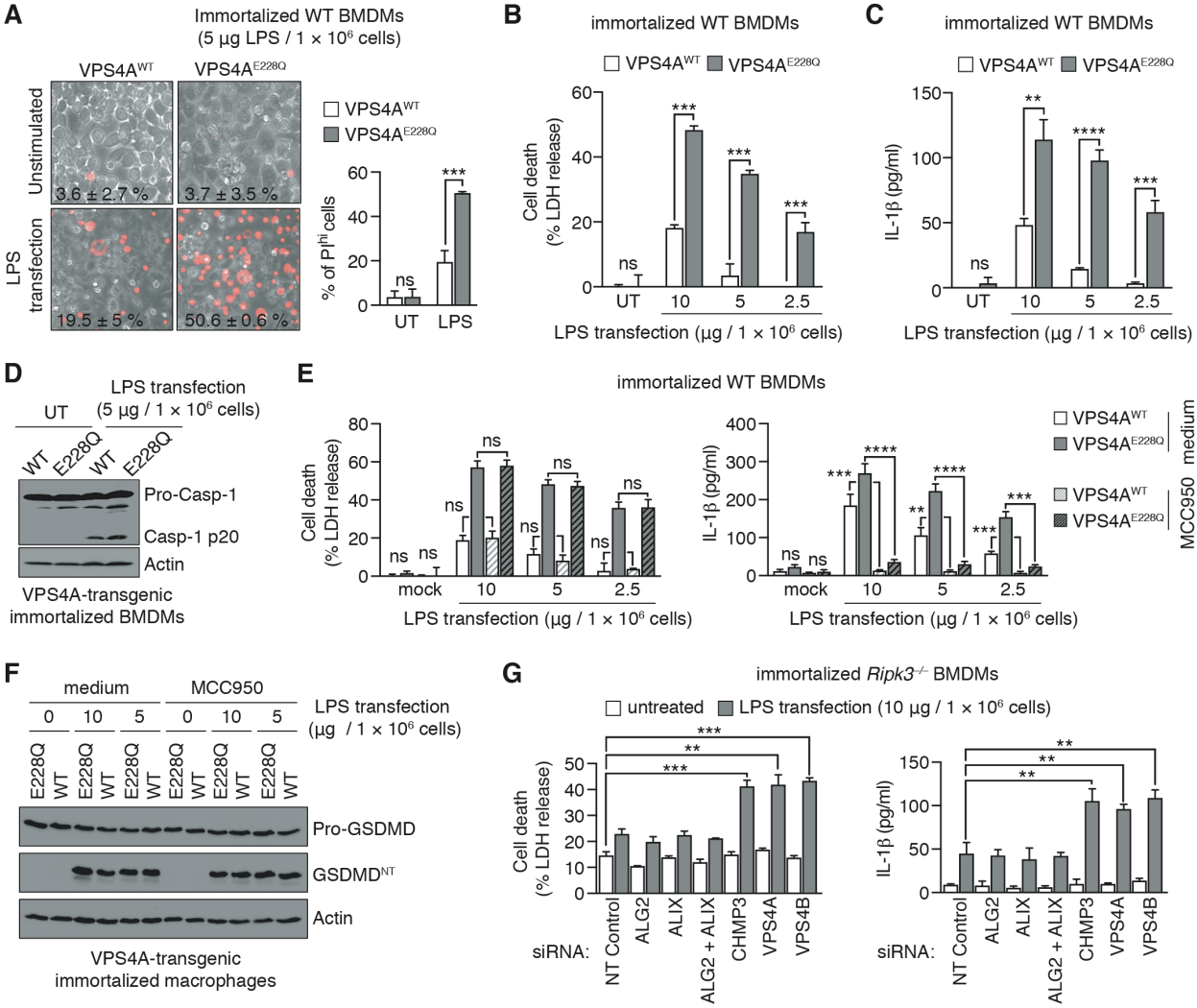

aar7670 Figure 4

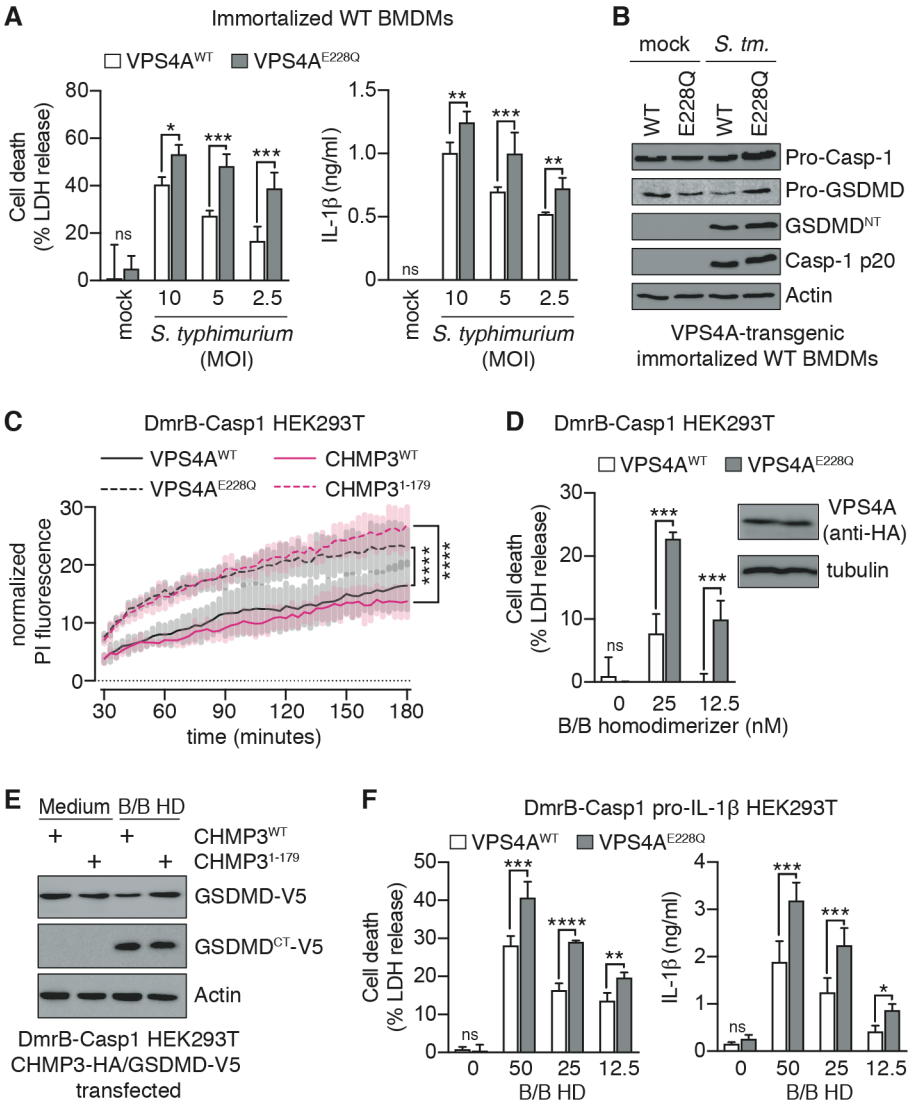

Supplementary Materials for

ESCRT-dependent membrane repair negatively regulates pyroptosis downstream of GSDMD activation

Sebastian Rühl, Kateryna Shkarina‡, Benjamin Demarco‡, Rosalie Heilig‡, José Carlos Santos‡ and Petr Broz*

* corresponding author: petr.broz@unil.ch

‡ these authors contributed equally

This PDF file includes:

Material and Methods

Figs. S1 to S18

Captions for Movies S1-S8

Other Supplementary Materials for this manuscript include the following:

Movies S1-S8

Materials and Methods

Cell culture. BMDMs were differentiated in DMEM (Sigma-Aldrich) with 10% v/v FCS (Amimed), 10% MCSF (L929 cell supernatant), 10 mM HEPES (Amimed), and nonessential amino acids (NEAA, Amimed). For seeding, medium was aspirated and replaced with 5 ml ice cold PBS. Dishes were incubated at 4 °C for 15 minutes, cells were lifted using a cell scraper (Sarstedt) and collected. Cells were centrifuged (200 × *g,* 5 min, 4 °C), resuspended in the specified assay medium (see below) and counted. Immortalized BMDMs (iBMDMs) were described previously and maintained in DMEM supplemented with 10% FCS, 10% 3T3-MCSF-conditioned medium and 1 × PenStrep (Amimed). HeLa and HEK 293T cells were cultured in DMEM with 5% FCS and 1 × PenStrep (Amimed). For retrovirally transduced cell lines, cells were cultured in medium with respective antibiotics until the day prior to an experiment.

Knock-down. Immortalized *Ripk3*$^{-/-}$ BMDMs were forward transfected with siRNA (30 pmol per 1 × 10^6 cells per well) in six-well plates using Lipofectamine RNAiMAX (Life technology) according to the manufacturer's instructions. Medium was replaced at 4 hours post-transfection for complete iBMDMs medium. After 48 hours, cells were reseeded into a 96-well plate (5 × 10^4 cells/well) for subsequent experiments and incubated for an additional 24 hours. RNAi efficiency was assessed by immunoblotting at 72 hours post-transfection. SiRNAs (siGenome SMARTpool) were purchased from Dharmacon: Non-Targeting siRNA Pool #2 (D-001206-14-05), CHMP3 siRNA (M-062411-01-0005), VPS4A siRNA (M-046156-00-0005), VPS4B siRNA (M-044487-01-0005), ALIX siRNA (M-062173-00-0005), ALG2 siRNA (M-062699-01-0005), Ptpn23 siRNA (M-062317-01-0005) and TSG101 siRNA (M-049922-01-0005).

LPS transfection. BMDMs or iBMDMs were seeded in assay medium (DMEM, 10% FCS, 10% 3T3-MCSF-conditioned medium, 10 mM Hepes and 1 × NEAA) 1 day prior to stimulation at a density of 3 × 10^4 (BMDMs) or 5 × 10^4 (iBMDMs) cells per well in 96-well plates and grown overnight at 37 °C and 5% CO_2. The next day, supernatant was removed and the cells were primed for 4 hours with 100 µl per well of 0.2 µg/ml Pam_3CSK_4 or 0.5 µg/ml LPS O55:B5 in complete medium. LPS/FuGeneHD complexes were prepared by mixing 100 µl Opti-MEM (Gibco) with ultrapure LPS O111:B4 (Invivogen) and 0.5 µl of FugeneHD (Promega) per 5 × 10^4 cells to be transfected. The transfection mixture was vortexed briefly, incubated for 5 minutes at room temperature and added dropwise to the

cells. Plates were centrifuged at for 5 minutes at 200 × *g* and 37 °C. Cells were incubated for indicated times at 37 °C and 5% CO_2 and cell death and IL-1β levels were determined as described below.

Stimulation of canonical inflammasomes. BMDMs and iBMDMs were seeded at a density of 5×10^4 cells per well of a 96-well plate and grown overnight in DMEM, 10 % FCS, 10 % 3T3-MCSF-conditioned medium, 10 mM Hepes, 1 × NEAA (complete medium). Cells were primed in complete medium with 500 ng/ml LPS (O55:B5, Invivogen) for 4 hours unless stated otherwise. Cells were washed once with PBS and 100 µl of Opti-MEM was added to each well. Stimuli were prepared in additional 100 µl of Opti-MEM to yield a final volume of 200 µl per well. *Salmonella enterica* serovar Typhimurium (referred to as *S. typhimurium)* SL1344 was grown to log phase (OD 1.4-1.8) in LB, diluted in Opti-MEM to the respective MOI and added to the cells. The plate was centrifuged for 5 minutes at 200 × *g*. Cells were incubated at 37 °C and 5% CO_2 for 45 to 60 minutes and samples were processed as required. Poly(dA:dT) (Invivogen) was transfected using 0.5 µg linear PEI (Polysciences, 1 mg/ml stock) by preparing desired amounts of poly(dA:dT) in 50 µl Opti-MEM per well and 10 µg/µl PEI separately. Fifty microliters of PEI solution was added to poly(dA:dT) solution and mixture was incubated 10 minutes at room temperature. One hundred microliters were added to cells and stimulation was carried out 1-3 hours prior to sample collection.

Inhibitor treatment. Cells were washed once with pre-warmed PBS and 100 µl of Opti-MEM supplemented with 2 × of the final inhibitor was added per well of a 96-well plate. Cells were pre-incubated at room temperature (BAPTA-AM) or 37 °C (MCC950) for 30-45 minutes. Medium for HeLa cells or iBMDMs was supplemented with 1 mM Probenecid (Sigma) to inhibit efflux of BAPTA-AM. Cells were subsequently treated with respective stimulus (LPS transfection, poly(dA:dT) transfection, *S. typhimurium*) prepared in 100 µl medium without inhibitor and added to cells to yield a final concentration of 1 × of the respective inhibitor. Volumes were scaled up accordingly for 12-well plates to prepare samples for SDS-PAGE analysis.

Cytokine and LDH release measurement. IL-1β was measured by ELISA (eBioscience). LDH was measured using LDH Cytotoxicity Detection Kit (Clontech). To normalize for spontaneous lysis, the percentage of LDH release was calculated as follows: (LDH treated – LDH untreated WT cells or medium control) / (LDH total lysis – LDH untreated WT cells or medium control) × 100. Plates were read using a Cytation 5 plate reader (BioTek).

Resazurin cell viability assay. Cells were washed once with pre-warmed PBS and incubated for 3 h with 100 µl iBMDMs medium supplemented with 16 µg/ml Resazurin (Sigma-Aldrich). Plates were read using a Cytation 5 plate reader (BioTek) according to the manufacturer's instructions. To determine percentage of cell viability values were normalized to untransfected cells.

ASC speck immunofluorescence. iBMDMs were plated at 2×10^5 cells per well in 24-well plates on sterile glass coverslips (13-mm diameter) in 1 ml of assay medium. Cells were allowed to attach overnight and cells were stimulated the next day as outlined above. After stimulation, coverslips were washed with PBS and fixed with 4% PFA at room temperature (RT) for 20 minutes. Following fixation, coverslips were washed with PBS and excess PFA was quenched using 100 mM glycine in PBS for 5 minutes. Coverslips were washed two times with PBS and permeabilized using 0.1% Triton (vol/vol) in PBS for 5 minutes. Coverslips were washed three times with PBS and coverslips were transferred to a humidity chamber and blocked with 200 µl of 5 % FCS in PBS for 1 h. Coverslips were stained with a monoclonal anti-ASC antibody (rat, 2 µg/ml, Genentech Inc.) in PBS containing 2% FCS for 1 hour at RT. Following staining, coverslips were washed three times 2 minutes with PBS and stained with an Alexa-568 conjugated anti-rat antibody (4 µg/ml, goat-anti-rat Alexa 568, life technologies, A11077) for 1 hour at RT in the dark. Coverslips were washed three times 5 minutes with PBS and mounted on glass slides using 2 µl Vectashield® mounting medium containing DAPI and sealed with nail polish. Slides were analyzed on a LSM700-Upright point scanning confocal microscope at 40 × magnification. Images were analyzed with Image-J, ASC specks and cells per field of view were counted manually. Four images (at least 100 cells per condition) from two coverslips were quantified per experiment.

Infection of HeLa cells and bacterial invasion assays. HeLa cells stably transduced with HA-tagged Dox-inducible VPS4A or CHMP3 were seeded at density of 2.5×10^4 cells per well in 96-well plates and protein expression was induced using 1.0 µg/ml Dox for 12 hours. Δ*sifA S. typhimurium* SL1344 was grown overnight in low salt LB medium supplemented with 20 µg/ml kanamycin (Sigma), sub-cultured 1:50 in fresh LB with kanamycin and grown for 3 hours until a late exponential phase (OD_{600} of 1.5). Bacteria were then added to the cells at the indicated MOIs and the plate was centrifuged for 5 minutes at 200 × *g* and 37 °C. Cells were incubated at 37°C for 30 minutes and gentamycin (Amimed) was added to a final concentration of 50 µg/ml to kill extracellular bacteria. After another 30 minutes, cells were washed once with warm medium and then fresh medium supplemented with 10 µg/ml gentamycin

was added. Infection was allowed to proceed for the indicated time points before cells were processed for LDH, immunoblot analysis or for enumeration of intracellular bacteria. To count the number of intracellular bacteria, infected cells were gently washed with PBS, lysed with distilled water containing 0.2% Triton X-100, and bacteria were then serially diluted and plated onto LB agar plates.

SCV rupture assays. HeLa cells stably transduced with HA-tagged Dox-inducible VPS4A or CHMP3 constructs were seeded one day before transfection with a plasmid encoding galectin3-eGFP, using the X-treameGENE 9 DNA Transfection Reagent (Roche) for 48 hours, according to the manufacturer's instructions. Protein expression was induced using 1.0 µg/ml Dox for 12 hours and cells were infected with Δ*sifA S. typhimurium* SL1344-expressing mCherry grown until a late exponential phase. Here, bacteria were added to the cells at a MOI of 100 and incubated for 10 min at 37°C, so that a synchronized infection could be followed. Non-internalized bacteria were washed three times with warm medium and incubated up to 30 min at 37°C, before extracellular bacteria were killed by adding medium containing 50 µg/ml gentamicin. At 1 h post-invasion, cells were washed with PBS, fixed with 4% PFA at RT for 20 minutes and imaged by confocal microscopy.

Cell lysis and immunoblotting. For immunoblots cells were plated and stimulated in 12-well plates at 5×10^5 cells per well. After stimulation/infection in Opti-MEM plates were transferred on ice and the supernatants were collected in a new tube. Cells were washed once with ice-cold PBS and lysed in RIPA buffer (150 mM NaCl, 1% NP40, 0.5% sodium deoxycholate and 0.1% SDS, pH 7.4). Lysates were transferred to new tubes and incubated for 15 minutes on ice. Subsequently lysates were centrifuged (21,000 × *g*, 10 min, 4 °C) and cytosolic extracts were transferred to new tubes. The protein concentration was determined by the BCA method, adjusted to the lowest concentration with water and diluted 1:4 with 5 × Laemmli buffer. Lysates were boiled for 5 minutes at 95 °C and stored at -20 °C until further processing. TCA was added to supernatants a final concentration of 5% (vol/vol) to precipitate proteins and supernatants were kept on ice for 15 minutes. Supernatants were centrifuged (21,000 × *g*, 10 min, 4 °C), and pellets were washed with 1 ml of ice-cold acetone and centrifuged again as above. Acetone was discarded and pellets were air-dried and resuspended in 1 × Laemmli buffer supplemented with 100 mM Tris and boiled at 95 °C for 10 minutes. If combined lysates and supernatants were analyzed, the protein concentration was not adjusted but precipitated protein pellets were resuspended in equal volumes of the respective cell lysates. Samples were processed for SDS-PAGE and immunoblotting.

Calcium and PI flux analysis. BMDMs were seeded in 8-well Ibidi treat® dishes (Ibidi) at 6×10^5 cells per well the day before the experiment. Cells were primed in complete medium with 0.2 µg/ml Pam_3CSK_4 for 4 hours. Cells were washed once with HBSS (Gibco) and incubated in the dark at room temperature for 45 minutes in HBSS supplemented with 4 µM Fluo-8 (Abcam, ab142773) in the presence of 2 mM Probenecid (Sigma). Cells were washed twice with HBSS and left either unstimulated or transfected with LPS as described above. HBSS was supplemented with 60 µM propidium iodide. After centrifugation, cells were transferred to "FEI More" wide field microscope (Field Electron and Ion Company), equipped with a heated stage, CO_2 supply and a Hamamatsu ORCA flash 4.0 cooled sCMOS camera. Cells were imaged every 30 seconds at 40 × magnification. After acquisition, single cells were segmented manually and analyzed for Fluo-8 and PI fluorescence using Fiji (https://imagej.net).

Live cell imaging. For live imaging experiments, DmrB-Caspase-1-transgenic HEK293T cells were seeded in 8-well tissue-culture treated slides (Ibidi) one day prior to transfection. Cells were transfected with 100 ng of plasmid DNA using JetPRIME transfection reagent (Polyplus transfection) accordingly to manufacturer's recommendations. For expression of proteins by doxycycline induction, medium was exchanged 8 hours post transfection and cells were treated with 1 µg/ml doxycycline for 16 hours. Live imaging experiments were performed using Zeiss LSM800 point scanning confocal microscope equipped with 63x Plan-Apochromat NA 1.4 oil objective, Zeiss ESID detector module, LabTek heating/CO2 chamber and motorized scanning stage. Prior to imaging, transfection medium was exchanged for HBSS (Gibco) supplemented with 2 % FCS, 1 % HEPES, 0.1 % cell culture antioxidant supplement (Sigma) and 70 ng/well Pacific Blue™ Annexin V (BioLegend). For the time-lapse experiments, each cell was imaged every 30 seconds at 63x magnification for 20 min in total, after which 2 µM (final concentration) of B/B homodimerizer was added directly to the well, and the same cells were imaged for additional 20 to 40 min. For the imaging of late stage pyroptotic cells, z-stacks of single cells were acquired approximately 1 hour post B/B homodimerizer addition.

Analysis of PI negative cells. Cells were segmented manually using Brightfield images and PI incorporation was quantified using Fiji. $(F_t\text{-}F_0)/F_0$ values of 15 unstimulated cells were calculated and an average of these values was calculated for each time point to correct for spontaneous flux of PI across the plasma membrane. $(F_t\text{-}F_0)/F_0$ of single, PI-negative cells from LPS-transfected conditions were calculated for each movie time point and the average PI value of the 15 unstimulated cells for the respective time point was subtracted to assess if enhanced PI incorporation caused by LPS transfection occurs. Curves were plotted for single cells as shown in the figures.

Lentiviral transduction. To produce lentiviral particles, 1×10^6 HEK 239T cells were transfected with 2 µg lentiviral plasmid, 2 µg psPax2, and 0.4 µg VSV-G for 6 hours. Medium was exchanged and lentiviral particles were collected 24 hours later. Two hundred fifty thousand cells were spin-infected with these particles and transduced cells were selected with appropriate antibiotic for 7 days. Selected cells were used for experiments.

HEK293T transfection and stimulation. Cells were seeded in polylysine-coated 96-well plates (40,000 cells per well) one day prior to transfection. Cells were subsequently transfected with 300 ng of plasmid DNA and 3 × (wt/vol) linear PEI. For expression of proteins by doxycycline treatment, the medium was exchanged 8 hours post-transfection and cells were treated with 1 µg/ml doxycycline for 16 hours. Twenty-four hours post-transfection, cells were stimulated as indicated in the respective figures.

HeLa infection. HeLa cells were seeded at density of 2.5×10^5 cells per well in 96-well plate one day prior to transfection. *Salmonella enterica* serovar Typhimurium (referred to as *S. typhimurium)* SL1344 Δ*sifA* was grown to stationary phase in low salt LB supplemented with 20 µg/ml kanamycin (Sigma). The overnight culture was sub-cultured 1:50 in fresh LB with kanamycin and grown for 3 hours until an OD_{600} of 1.5 was reached. HeLa cells were infected with the indicated MOIs and the plate was centrifuged for 5 minutes at 200 × *g* and 37 °C. After 30 minutes gentamycin (Amimed) was added to a final concentration of 50 µg/ml to kill the extracellular *Salmonella*. After another 30 minutes, cells were washed once with PBS and then fresh medium supplemented with 10 µg/ml gentamycin was added. Infection was allowed to proceed for another 4 hours before cells were processed for LDH or immunoblot analysis.

Expression of ESCRT wildtype and dominant-negative proteins. Human CHMP3 and VPS4A were amplified from cDNA and cloned into pRetroX Tet-On 3G (Clontech). GP2 packaging cells (Clontech) were transfected with the respective plasmids and VSV-G at a ratio of 8:1 using three times (wt/vol) PEI. Retroviral particles were collected after 36 and 72 hours, combined and cells were transduced by spin-infection (1,900 × *g*, 90 minutes). After two days, transduced cells were selected by puromycin selection for 6 days. Experiments were conducted with pools.

Antibodies. Primary antibodies used (Manufacturer, Catalogue N°): polyclonal rabbit anti-ASC at 1 µg/ml (Adipogen AG-25B-0006), monoclonal mouse anti-HA at 1:1000 dilution (Enzo Life Science, ENZ-ABS-118-0200), anti-FLAG at 2 µg/ml (Stratagene, 200472-21), anti-caspase-1 p20 at 1 µg/ml (Adipogen, AG20B-0042), anti-GAPDH at 1:10000 (Thermo scientific, AM4300), anti-V5 at 1:5000 (Thermo Scientific, R960-25), anti-actin at 1:20000 (Merck,

MAB1501), rabbit anti-gasdermin-D, at 0.6 μg/ml (Abcam ab209845), anti-RIPK3 at 1 μg/ml (rabbit; no. IMG-5523-2, Imgenex); anti-VPS4A at 1.3 μg/ml (mouse; no. ab213526, Abcam); anti-VPS4B at 5 μg/ml (rabbit; no. ab224736, Abcam); anti-CHMP3 at a 1000-fold dilution (rabbit; no. ab175930, Abcam); anti-ALG2 at 0.0108 μg/ml (rabbit; no. ab133326, Abcam); anti-ALIX at a 1000-fold dilution (rabbit; no. pab0204, Covalab); anti-Tubulin at 0.1 μg/ml (rabbit; no. ab4074, Abcam).

Densitometric quantification of western blots. Equal ROIs were used to quantify the processed form of GSDMD or caspase-1 using Fiji. For all conditions loading controls (e.g. actin, tubulin or gapdh) were quantified using Fiji. For not stimulated conditions unprocessed forms of proteins were normalized to loading controls (Ratio A), for stimulated conditions the processed form was normalized to loading controls (Ratio B). Subsequently the Ratio B of each stimulated condition was normalized to the respective Ratio A. In a second step, the ratio of medium-treated samples or ESCRT-WT proteins compared to BAPTA-AM-treated or ESCRT-DN samples were determined for each condition in order to compare different experimental repeats.

Statistical analysis. Statistical tests were performed as described in the figure legends using GraphPad Prism 7 (GraphPad Software, Inc., La Jolla, CA, USA).

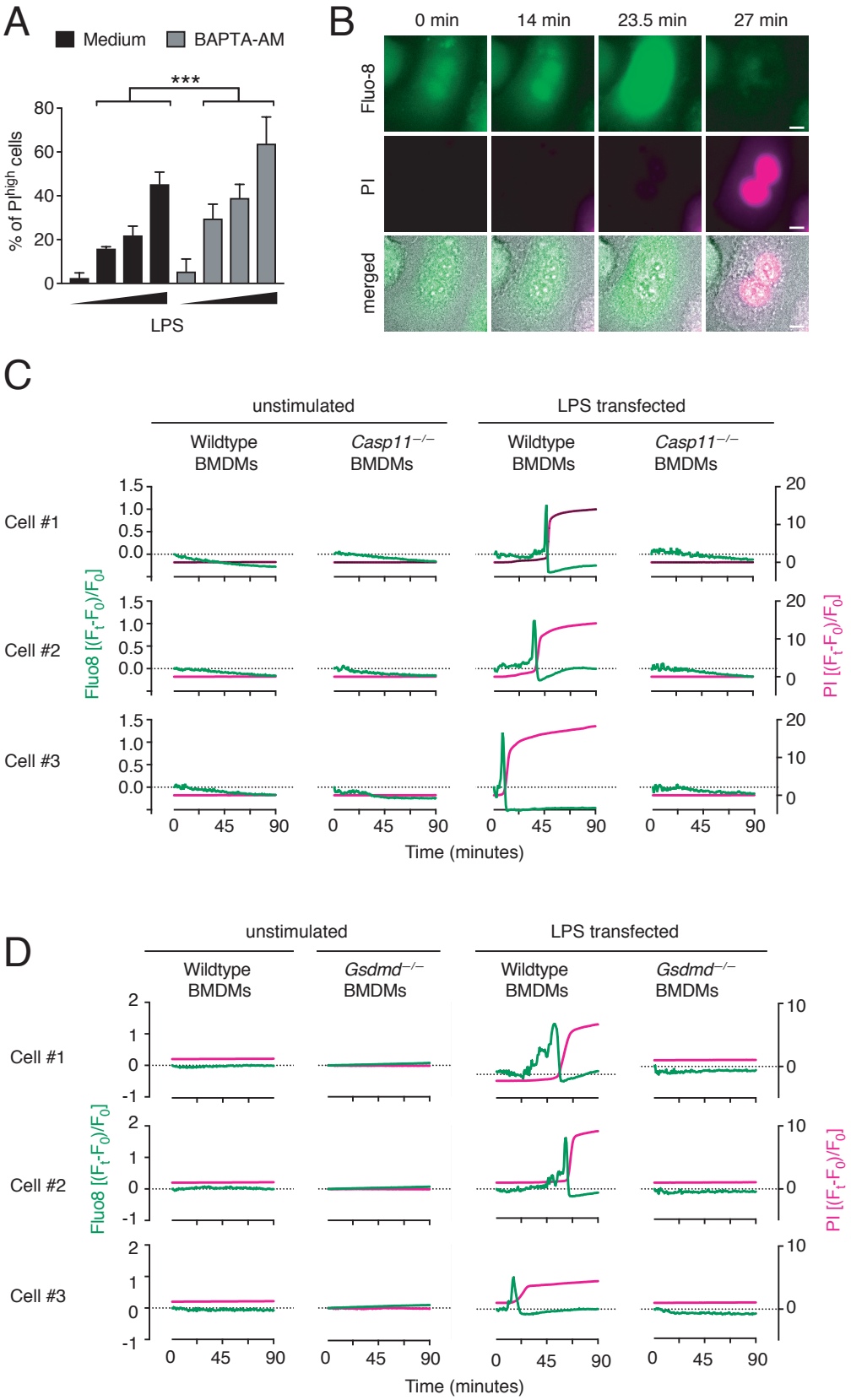
A
Medium
BAPTA-AM
***
% of PI^high cells
LPS
B
0 min
14 min
23.5 min
27 min
Fluo-8
PI
merged
C
unstimulated
LPS transfected
Wildtype BMDMs
Casp11−/− BMDMs
Cell #1
Cell #2
Cell #3
Fluo8 [(Ft-F0)/F0]
PI [(Ft-F0)/F0]
Time (minutes)
D
unstimulated
LPS transfected
Wildtype BMDMs
Gsdmd−/− BMDMs
Cell #1
Cell #2
Cell #3
Fluo8 [(Ft-F0)/F0]
PI [(Ft-F0)/F0]
Time (minutes)

Fig. S1. Ca^{2+} and PI influx measurements after non-canonical inflammasome activation.

A. Percentage of PI^{high} wildtype mouse BMDMs 2 hours after transfection with increasing amounts of LPS (0, 4.15, 8.3 or 16.6 µg / 1 × 10^6 cells) in absence or presence of 3.3 µM BAPTA-AM. Cells were primed with LPS for 4 hours before transfection. Three fields of view were analyzed and PI^{hi} cells enumerated manually. **B.** Time lapsed microscopy images of Ca^{2+} influx (Fluo-8) and membrane permeabilization (PI) in LPS-primed wildtype BMDMs after transfection of LPS (3.5 µg / 1 × 10^6 cells). Scale bars correspond to 5 µm. **C-D**. Single-cell analysis of Ca^{2+} (Fluo-8) and PI influx in LPS-primed wildtype, *Casp11*$^{-/-}$ and *Gsdmd*$^{-/-}$ BMDMs either unstimulated or transfected with LPS (3.5 µg / 1 × 10^6 cells). Graphs show three representative cells out of 25-30 analyzed per condition. See Material and Methods section for a detailed description of the calculation of Fluo-8 and PI intensity. Graphs show mean ± SD. ***P<0.001; Two-way ANOVA. Results are representative of at least three independent experiments.

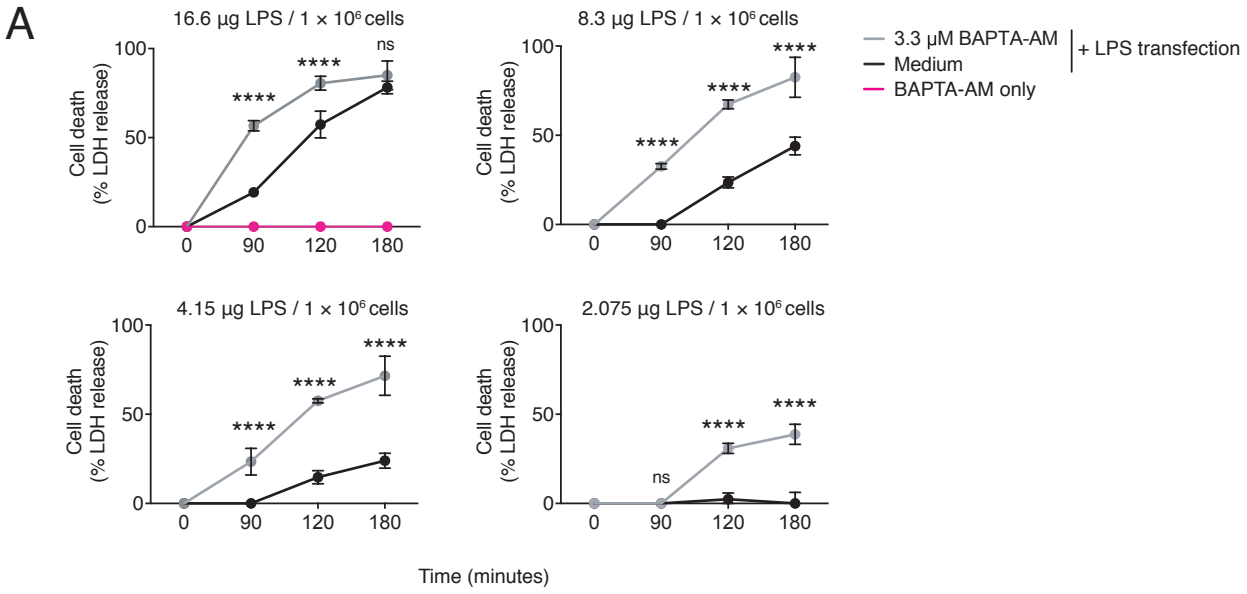

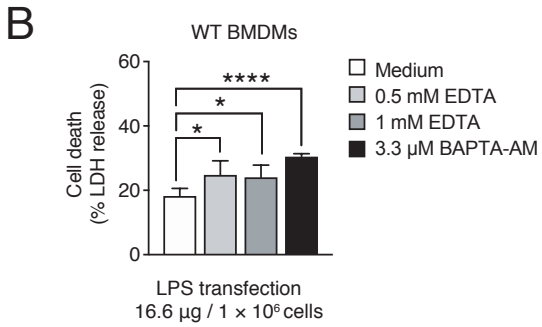

Fig. S2. Ca^{2+} chelation enhances cell death after non-canonical inflammasome activation and permits cell survival at sub-lethal levels of LPS transfection.

A. LDH release from LPS-primed wildtype mouse BMDMs after transfection with the indicated amounts of LPS in the presence or absence of 3.3 µM BAPTA-AM. BAPTA-AM control is only shown in first panel. **B.** LDH release from LPS-primed wildtype mouse BMDMs after transfection with 16.6 µg LPS per 1 × 10^6 cells for 2.5 hours in medium or in medium supplemented with the indicated amounts of Ca^{2+} chelators. Graphs show mean ± SD. **P*<0.05; *****P*<0.0001; ns, not significant; student's t-test. Results are representative of at least three independent experiments.

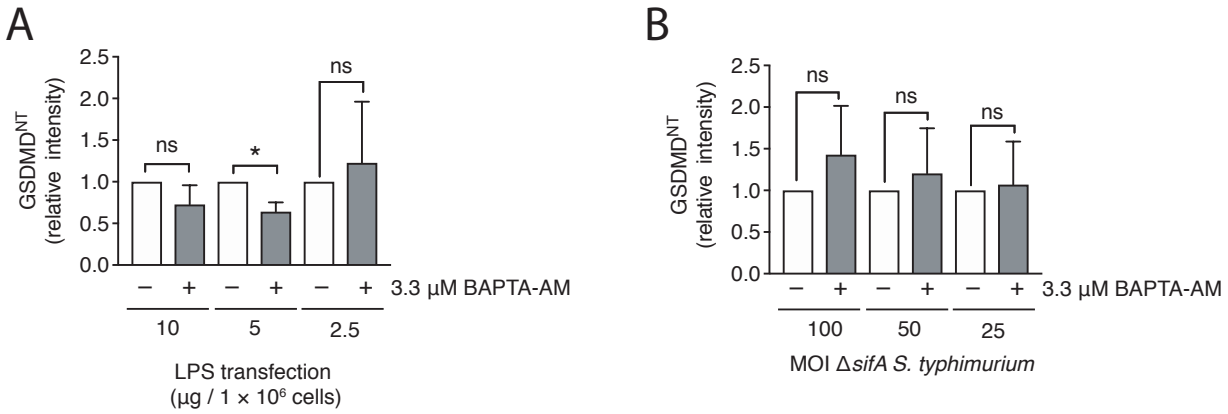

Fig. S3. Quantitative analysis of immunoblots from Figure 1E and 1G.

Densitometric quantification (as described in Material and Methods) of the processed $GSDMD^{NT}$ band in untreated or BAPTA-AM-treated HA-GSDMD-transgenic immortalized wildtype BMDMs 2 hours post LPS transfection (**A**) or untreated or BAPTA-AM-treated HeLa cells infected with Δ*sifA S. typhimurium* at the indicated MOIs for 5 hours (**B**). Results show combined data of n=3 repeats. Results are expressed as intensity relative to untreated control. **P*<0.05; ns, not significant; student's t-test.

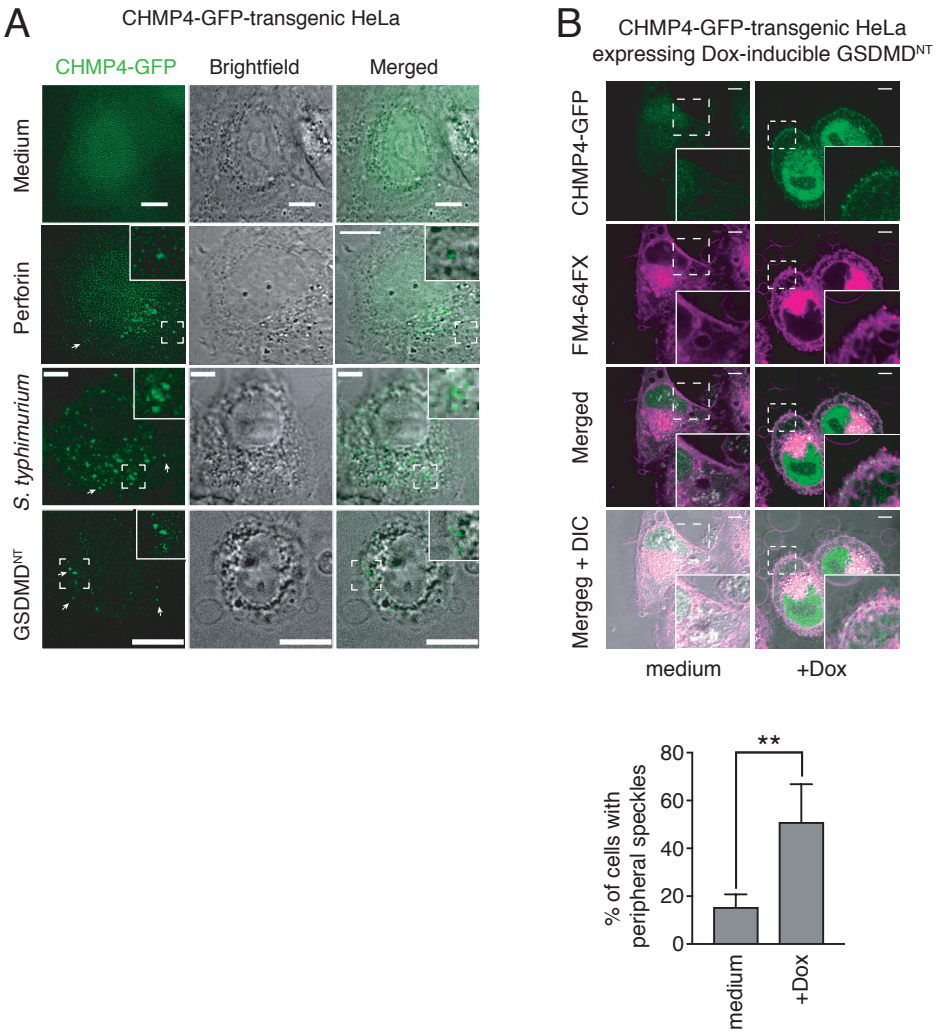

Fig. S4. CHMP4-GFP localizes to the plasma membrane upon pyroptosis induction.

A. Fixed cell microscopy images of CHMP4-GFP-transgenic HeLa cells left untreated, treated with perforin (control) (200 µg/ml, 45 minutes), infected with Δ*sifA S. typhimurium* (MOI 100, 5 hours) or expressing GSDMD^{NT} from Dox-inducible promoter (1 µg/ml Dox, 4 hours). **B.** Fixed-cell microscopy images and quantification of CHMP4-GFP puncta from CHMP4-GFP/Dox-inducible GSDMD^{NT} double-transgenic HeLa cells either left untreated or treated with Dox (1 µg/ml) for 4.5 hours. Membranes were stained with FM4-64FX. Scale bars correspond to 5 µm. Graphs show mean ± SD. ***P*<0.01; student's t-test Results are representative of at least three independent experiments.

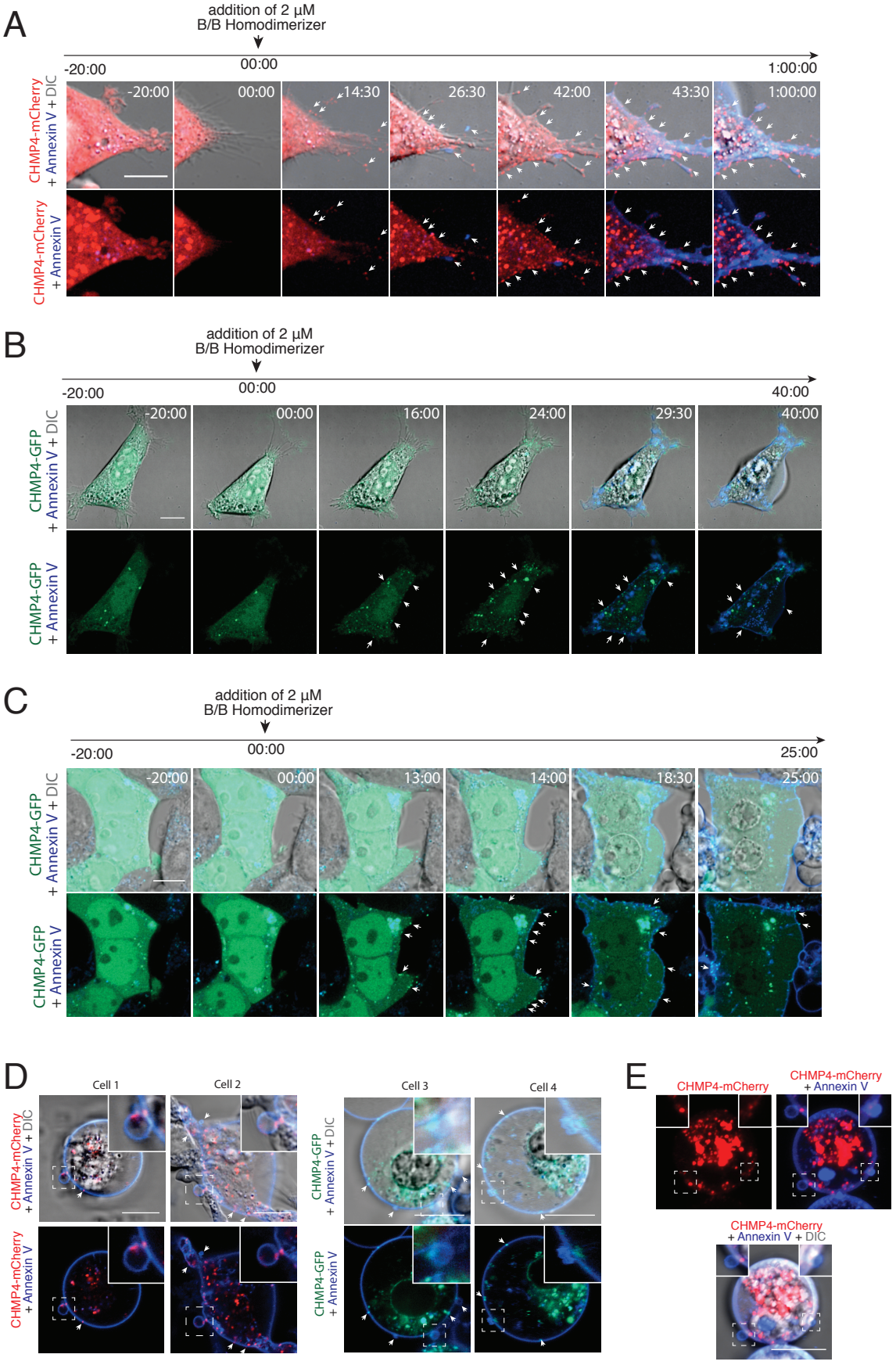
A
addition of 2 µM
B/B Homodimerizer
-20:00
00:00
1:00:00
CHMP4-mCherry
+ Annexin V + DIC
CHMP4-mCherry
+ Annexin V
-20:00
00:00
14:30
26:30
42:00
43:30
1:00:00
B
addition of 2 µM
B/B Homodimerizer
-20:00
00:00
40:00
CHMP4-GFP
+ Annexin V + DIC
CHMP4-GFP
+ Annexin V
-20:00
00:00
16:00
24:00
29:30
40:00
C
addition of 2 µM
B/B Homodimerizer
-20:00
00:00
25:00
CHMP4-GFP
+ Annexin V + DIC
CHMP4-GFP
+ Annexin V
-20:00
00:00
13:00
14:00
18:30
25:00
D
Cell 1
Cell 2
Cell 3
Cell 4
CHMP4-mCherry
+ Annexin V + DIC
CHMP4-mCherry
+ Annexin V
CHMP4-GFP
+ Annexin V + DIC
CHMP4-GFP
+ Annexin V
E
CHMP4-mCherry
CHMP4-mCherry
+ Annexin V
CHMP4-mCherry
+ Annexin V + DIC

Fig. S5. Localization of CHMP4 in HEK293T cells after activation of DmrB-Casp-1

A. Time-lapsed confocal images of high-level CHMP4-mCherry-expressing DmrB-Casp-1-transgenic HEK293T cells stained with Annexin-V as membrane marker. **B-C.** Time-lapsed confocal images of low level (**B**) and high level (**C**) CHMP4-GFP-expressing DmrB-Casp-1-transgenic HEK293T cells stained with Annexin-V as membrane marker. **D-E.** Confocal images of CHMP4-mCherry- or CHMP4-GFP-expressing DmrB-Casp-1-transgenic HEK293T cells stained with Annexin-V as membrane marker after 1 hour B/B homodimerizer treatment (2 μM) (late stage pyroptosis). Insets show Annexin-V-positive budding vesicles. Arrows show CHMP4 puncta. Scale bars are 5 (A) and 10 (B-D) μm.

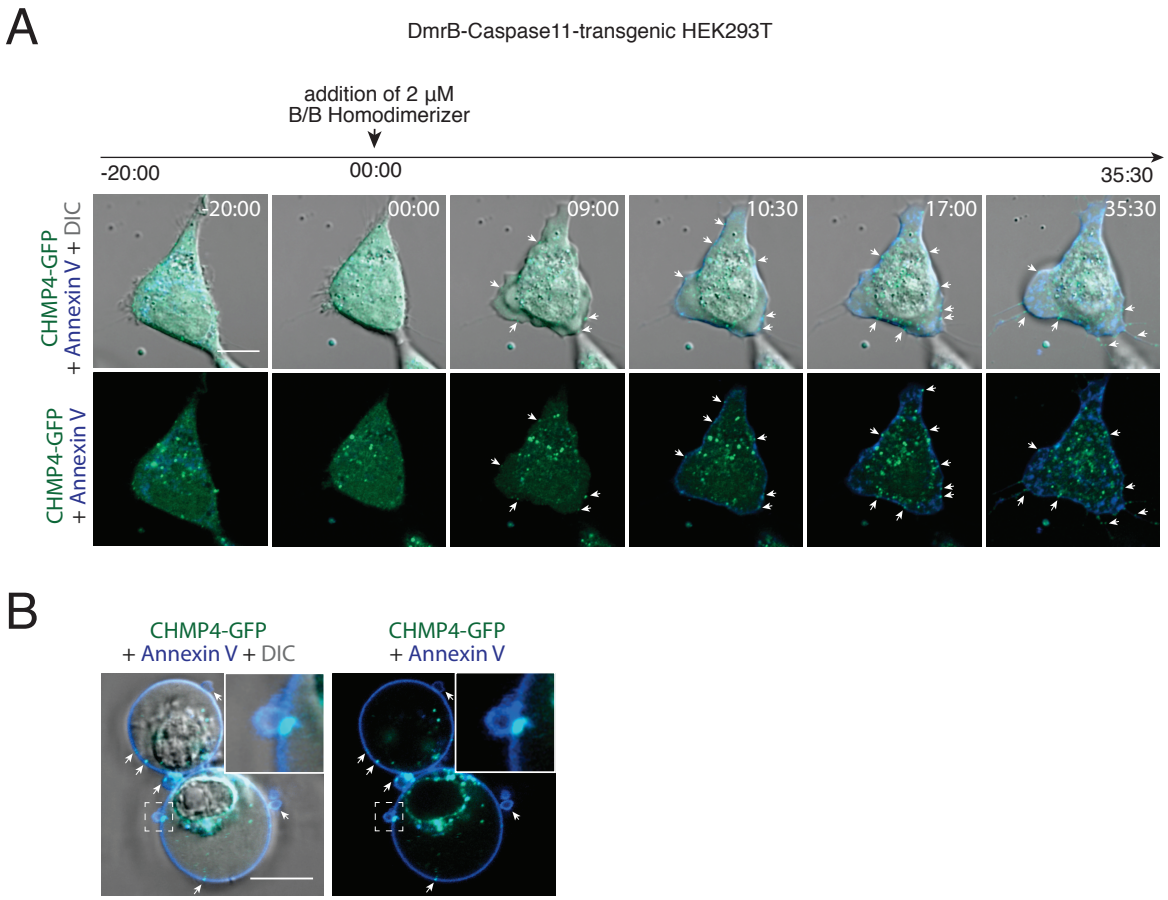

Fig. S6. Localization of CHMP4 in HEK293T cells after activation of DmrB-Casp-11.

A. Time-lapsed confocal images of CHMP4-GFP-expressing DmrB-Casp-11-transgenic HEK293T cells stained with Annexin-V as membrane marker. **B.** Confocal images of CHMP4-GFP-expressing DmrB-Casp-11-transgenic HEK293T cells stained with Annexin-V as membrane marker after 1 hour B/B homodimerizer treatment (2 μM) (late stage pyroptosis). Insets show Annexin-V-positive budding vesicles. Arrows show CHMP4 puncta. Scale bars are 10 μm.

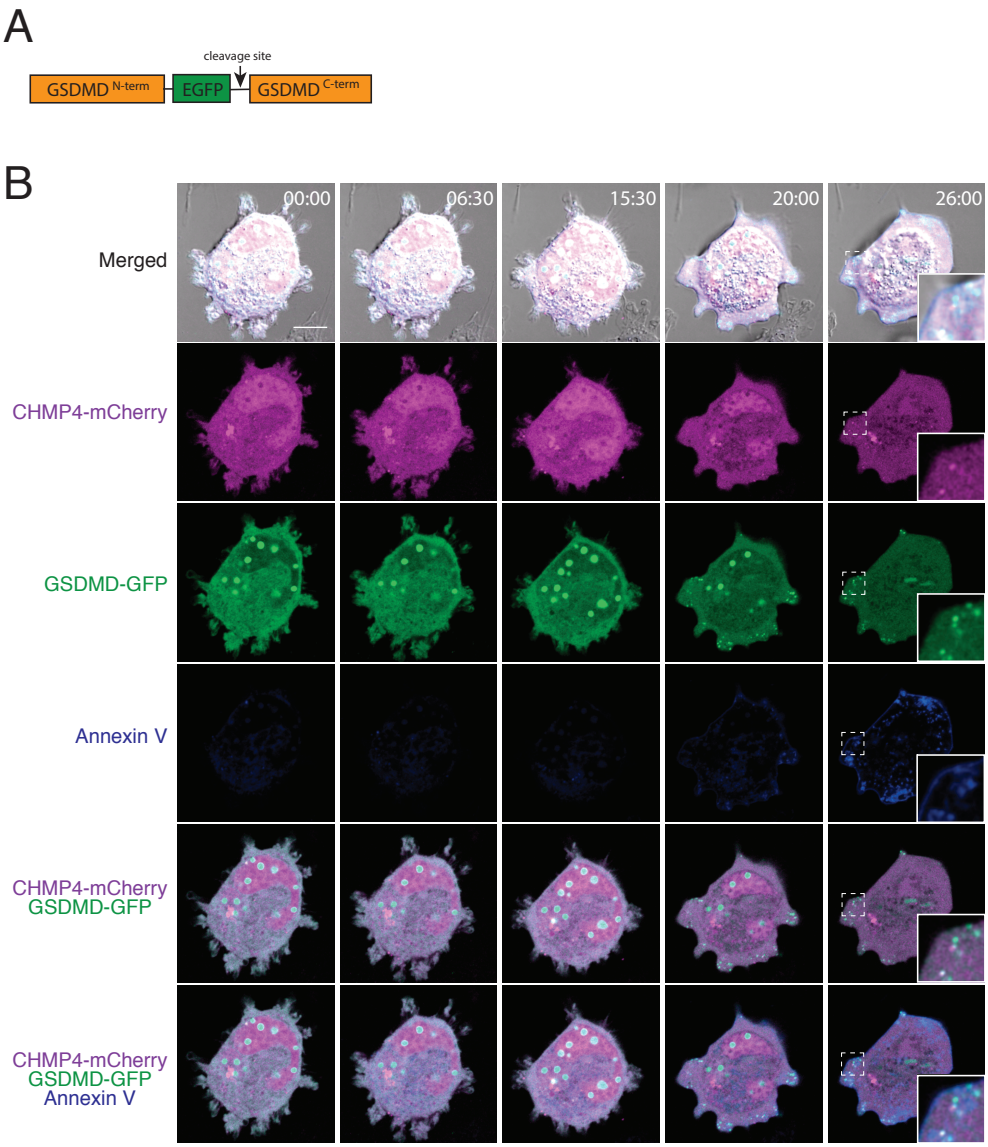
A
cleavage site
GSDMD N-term
EGFP
GSDMD C-term
B
00:00
06:30
15:30
20:00
26:00
Merged
CHMP4-mCherry
GSDMD-GFP
Annexin V
CHMP4-mCherry
GSDMD-GFP
CHMP4-mCherry
GSDMD-GFP
Annexin V
C
CHMP4-mCherry
GSDMD-GFP
CHMP4-mCherry
GSDMD-GFP
CHMP4-mCherry
GSDMD-GFP
Annexin V
Merged

Fig. S7. Localization of GSDMD during pyroptosis.

A. Schematic outline of the expression construct for mouse GSDMD with internal GFP-tag (referred to as GSDMD-GFP^{internal}). GFP tag was inserted between GSDMD^{NT} and the linker region so that a GFP-tagged GSDMD^{NT} is generated after cleavage. Of note, mouse GSDMD cannot be tagged N-terminal without loss of its pore-forming ability, since N-terminal residues are critical for membrane insertion and pore formation. **B.** Time-lapsed confocal images of CHMP4-mCherry- and GSDMD-GFP^{internal}-expressing DmrB-Casp-1-transgenic HEK293T cells stained with Annexin-V as membrane marker. B/B homodimerizer was added at 2 μM final concentration at t=0. Insets show close proximity of GSDMD and CHMP4 at peripheral regions. **C.** Examples of CHMP4-mCherry and GSDMD-positive vesicles shed from CHMP4-mCherry- and GSDMD-GFP^{internal}-expressing DmrB-Casp-1-transgenic HEK293T after B/B homodimerizer treatment. Scale bars are 10 (B) and and 1 (C) μm.

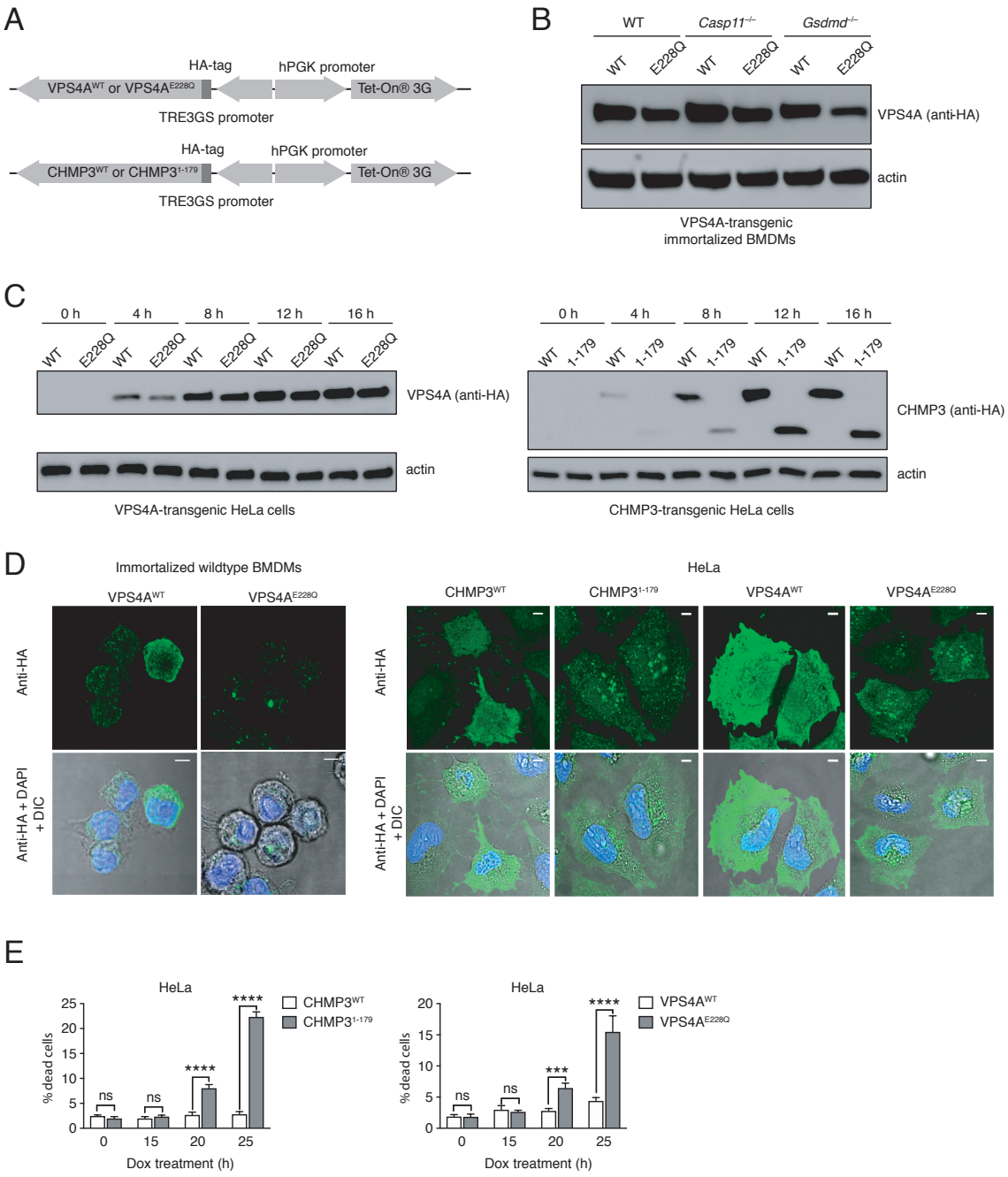

Fig. S8. Generation and characterization of VPS4A-transgenic iBMDMs and VPS4A-/CHMP3-transgenic HeLa cells

A. Schematic outline of pRetroX-Tet-On 3G plasmids used for the generation of cell lines with doxycycline (Dox)-inducible expression of HA-tagged wild-type and dominant negative human CHMP3 and VPS4A. **B.** Expression of VPS4A^{WT} or VPS4A^{E228Q} in lysates of VPS4A-transgenic iBMDMs wildtype, *Casp11*$^{-/-}$ or *Gsdmd*$^{-/-}$ BMDMs from Fig. 3C and 3E after induction for 6 hours with 0.5 µg/ml Dox. Immunoblots show anti-HA and anti-actin (loading

control). **C.** Time course of protein expression of HA-tagged $CHMP3^{WT}$, $CHMP3^{1-179}$, $VPS4A^{WT}$ or $VPS4A^{E228Q}$ in HeLa cells transgenic for Dox-inducible VPS4A or CHMP3 constructs after Dox treatment (1.0 µg/ml). Immunoblots show anti-HA and anti-actin (loading control). **D.** Subcellular distribution of wild-type and dominant-negative VPS4A or CHMP3 proteins in iBMDMs or HeLa cells from Fig. S7B-C. Cell lines were treated with 1 µg/ml Dox for 6 hours, fixed and stained for the HA-tag. Scale bars correspond to 5 µm. **E.** Cell viability measurement of HeLa stably transduced with Dox-inducible constructs for $CHMP3^{WT}$, $CHMP3^{1-179}$, $VPS4A^{WT}$ or $VPS4A^{E228Q}$ after Dox treatment for up to 25 hours. Cells were stained with a live/dead marker and cell death was quantified by flow cytometry analysis. Graphs (E) show mean ± SD. ***P<0.001; ****P<0.0001; ns, not significant; student's t-test. Results are representative of at least two independent experiments.

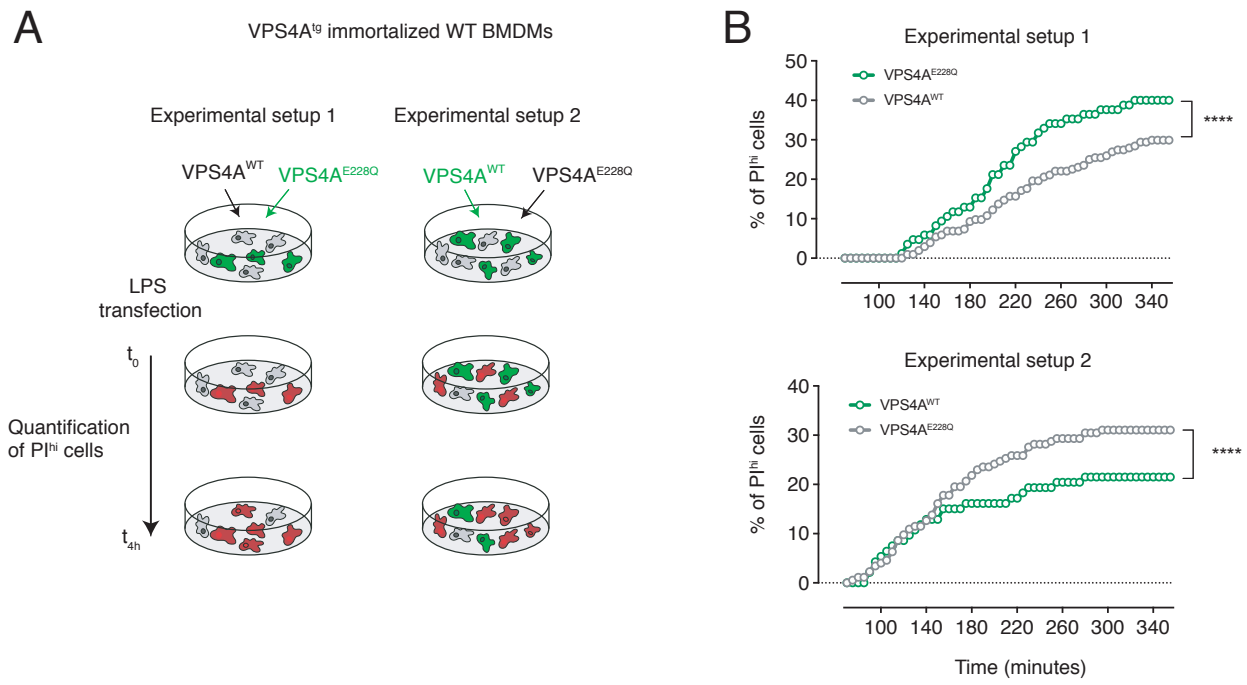

Fig. S9. Single-cell-based analysis of cell death in ESCRT-proficient and -deficient cells.

A. Schematic outline of the experimental setup: VPS4A^{WT} and VPS4A^{E228Q}-transgenic immortalized WT macrophages are seeded to equal ratio into iBidi chamber wells. In experimental setup 1, VPS4A^{E228Q}-transgenic immortalized WT macrophages express GFP to distinguish them from VPS4A^{WT}-expressing cells. In experimental setup 2, the VPS4A^{WT}-expressing cells express GFP and VPS4A^{E228Q}- expressing cells are unlabeled. Cells are transfected with LPS (5 µg/ml) for 1 hour, before changing to imaging medium (HBSS) and imaging for up to 4 hours. **B.** Percentage of PI^{hi} VPS4A^{WT} and VPS4A^{E228Q}-transgenic immortalized WT macrophages in experimental setup 1 or 2 over time. Representatives movies: Movie file 7 and 8. ****P<0.0001; two-way ANOVA. Results are representative of at least two independent experiments.

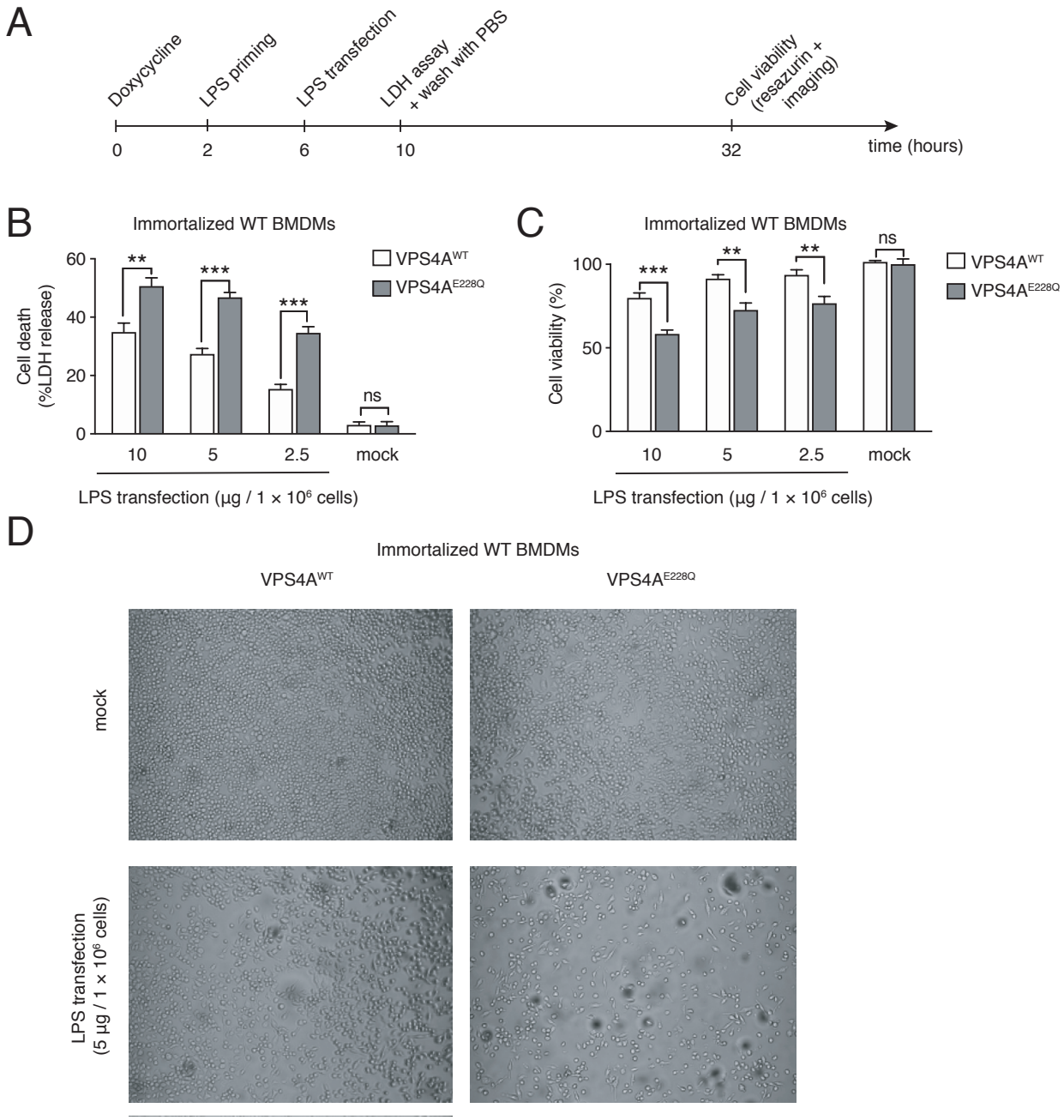

Fig. S10. ESCRT inhibition reduces long-term viability after LPS transfection.

A. Schematic outline of the long-term viability assay: VPS4A^{WT}- or VPS4A^{E228Q}-transgenic WT iBMDMs were primed with LPS (500 ng/ml) 2 hours after VPS4A^{WT}- or VPS4A^{E228Q} expression was induced by addition of 0.5 µg/ml doxycycline. Four hours later, cells were left untransfected or transfected with 2.5-10 µg LPS per 1 × 10^6 cells. **B.** Supernatant were removed and processed for LDH analysis at 4 hours post transfection. **C-D.** Cells were thereafter washed with PBS to remove LPS, doxycycline and transfection reagent and fresh medium was added. Twenty-four

hours later, cell viability was assessed using resazurin (**C**) and representative images were acquired (**D**). Graphs show mean ± SD. ***P* <0.01; ****P*<0.001; ns, not significant; student's t-test. Results are representative of at least two independent experiments.

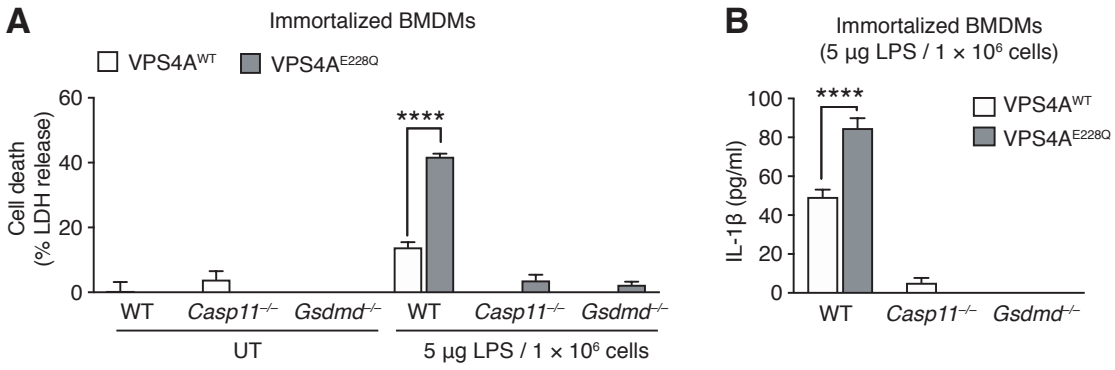

Fig. S11. Enhanced LPS-induced cell death after ESCRT inactivation requires Caspase-11 and GSDMD.

A-B. LDH and IL-1β release from VPS4A^{WT}- or VPS4^{AE228Q}-transgenic iBMDMs 2 hours after LPS transfection. Graphs show mean ± SD. ****P<0.0001; Student's t-test. Results are representative of at least three independent experiments. VPS4AWT/E228Q expression was induced with 0.5 µg/ml of Dox for 6 hours.

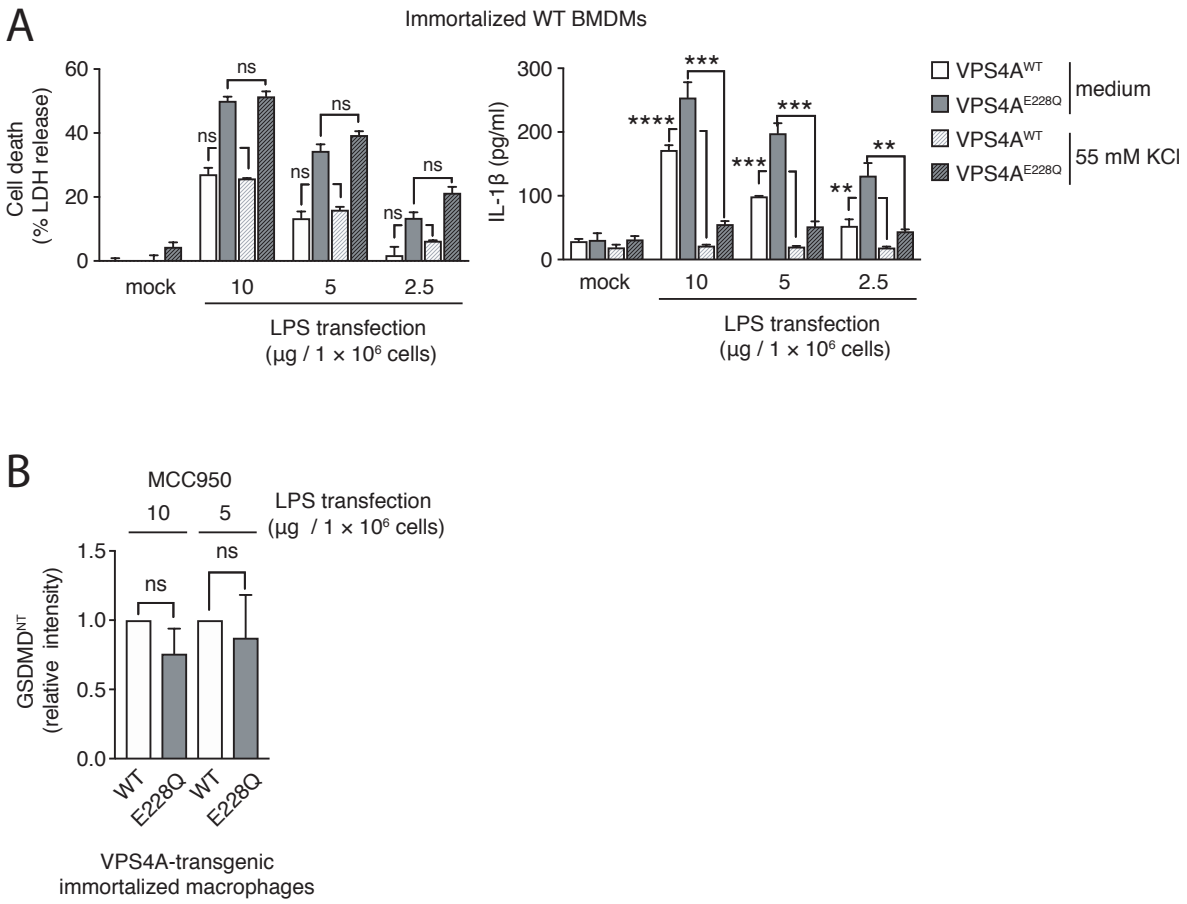

Fig. S12. Potassium efflux controls IL-1β release after LPS transfection in LPS-primed iBMDMs expressing VPS4A^{WT} or VPS4A^{E228Q}.

A. LDH and IL-1β release from VPS4A^{WT}- or VPS4A^{E228Q}-transgenic iBMDMs after LPS transfection for 2 hours in the presence or absence of 55 mM extracellular KCl. **B.** Densitometric quantification (as described in Material and Methods) of the processed GSDMD^{NT} band in VPS4A^{WT} or VPS4A^{E228Q}-expressing immortalized WT BMDMs 2 hours post LPS transfection in presence of MCC950. Results show combined data of n=3 repeats. Results are expressed as intensity relative to the GSDMD^{NT} in VPS4A^{WT}-expressing immortalized WT BMDMs. The representative immunoblot is shown in Figure 3F. Graphs show mean ± SD. ***P* <0.01; ****P*<0.001; *****P*<0.0001; ns, not significant; student's t-test. Results are representative of at least three independent experiments.

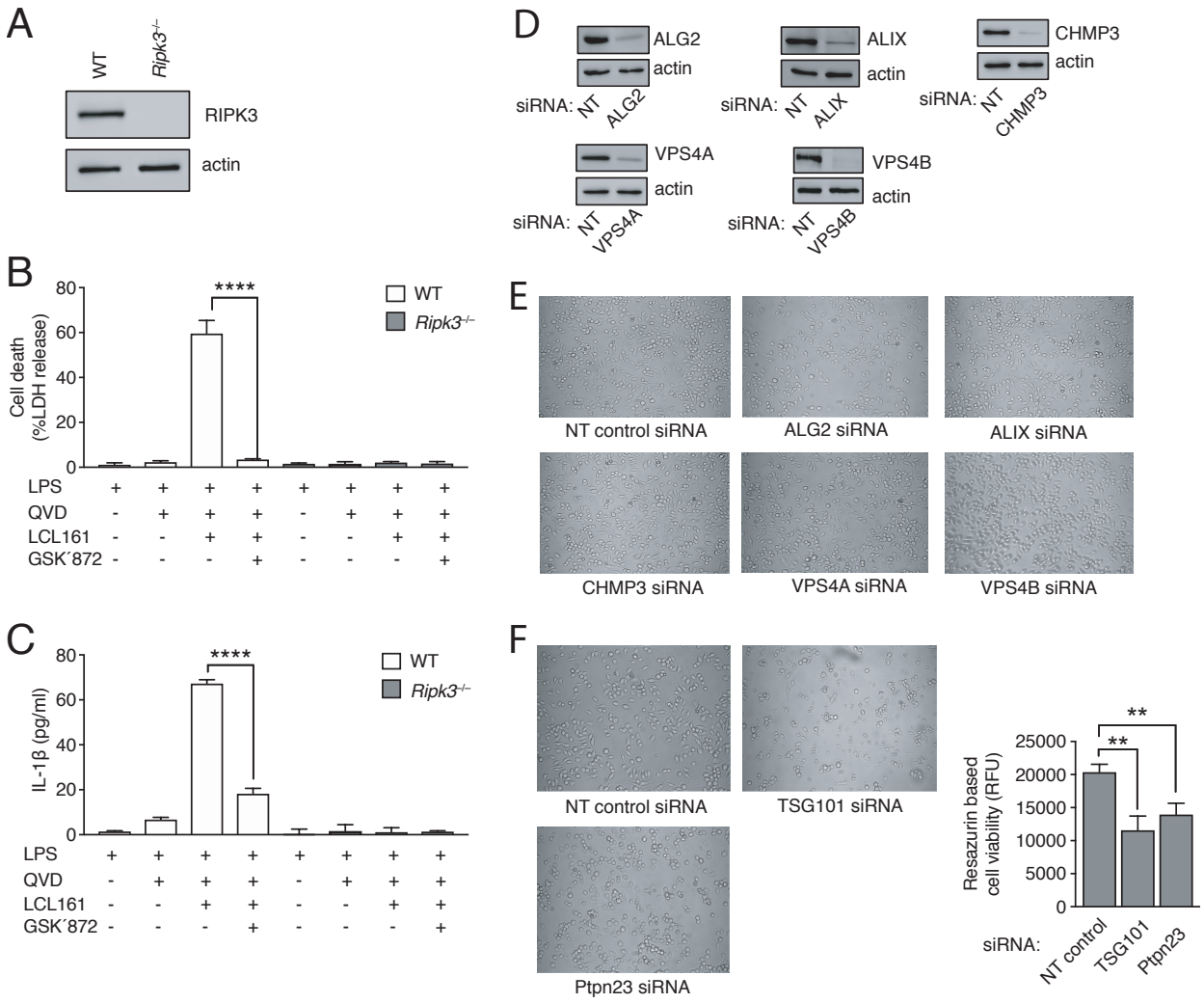

Fig. S13. Knock-down of ESCRT and ESCRT-associated proteins in *Ripk3*$^{-/-}$ iBMDMs.

A-C. Characterization of immortalized *Ripk3*$^{-/-}$ BMDMs showing (A) immunoblots for RIPK3 and actin (control) in WT and *Ripk3*$^{-/-}$ iBMDMs, and (B-C) LDH and IL-1β release from WT or *Ripk3*$^{-/-}$ iBMDMs primed with LPS (500 ng/ml) and treated with a combination of the pan-caspase inhibitor QVD (10 μM) and the SMAC mimetic LCL161 (4 μM) to induce necroptosis. Rip3 inhibitor GSK'872 was used at 1 μM to block necroptosis induction. **D.** Immunoblots for ALIX, ALG2, CHMP3, VPS4A, VPS4B and actin (control) in *Ripk3*$^{-/-}$ iBMDMs transfected with non-targeting (NT) siRNA or siRNA for ALIX, ALG-2, CHMP3, VPS4A or VPS4B. Immunoblots were done at 72 hours post-transfection. **E.** Images showing *Ripk3*$^{-/-}$ iBMDMs from A. **F.** Images and resazurin-based cell viability assay of *Ripk3*$^{-/-}$ iBMDMs transfected with non-targeting (NT) siRNA or siRNA for TSG101 or *Ptpn23* for 72 hours.

Graphs show mean ± SD. **P<0.01, ****P<0.0001; student's t-test. Results are representative of at least two independent experiments.

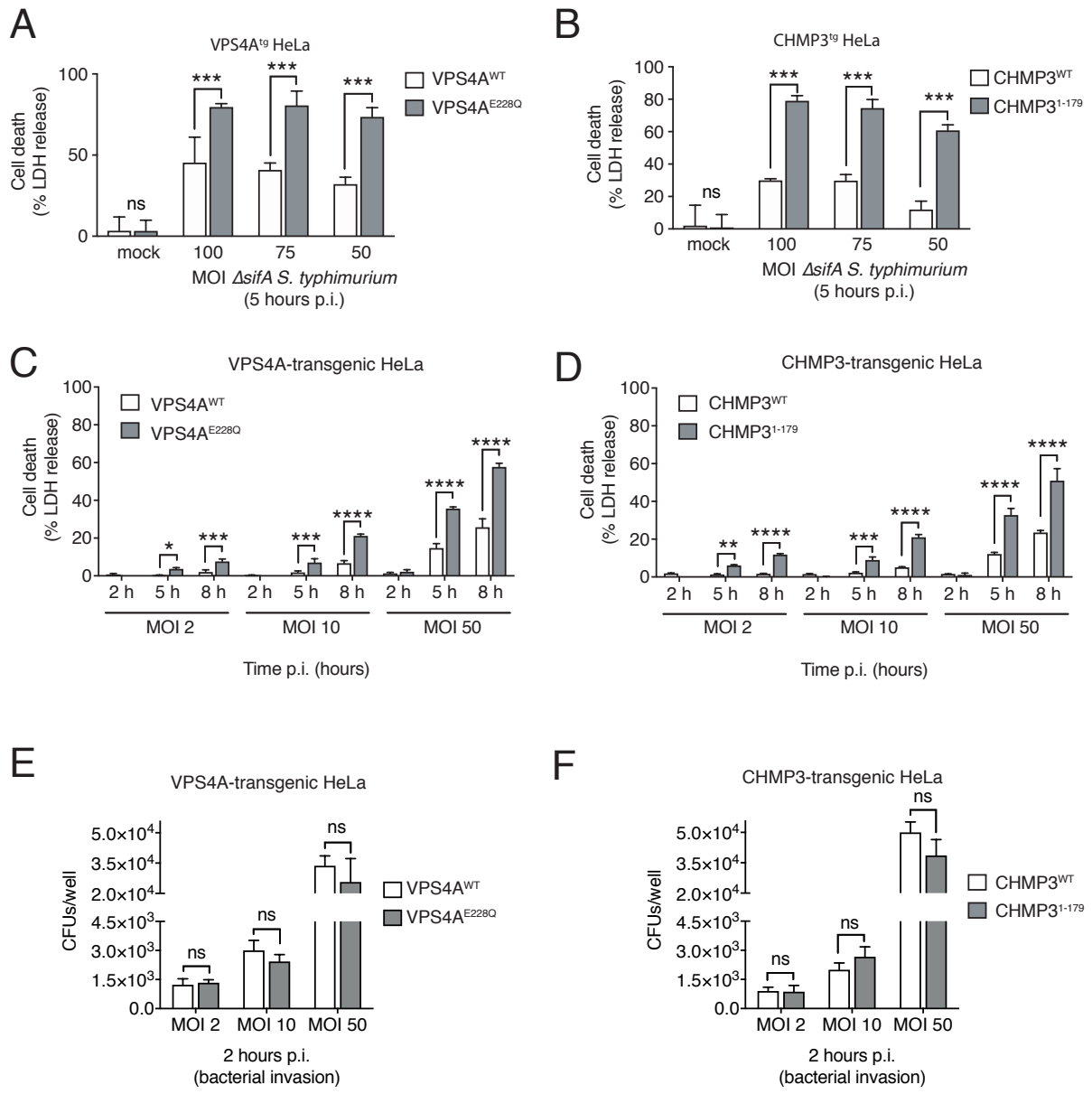

Fig. S14. ESCRT negatively regulates GSDMD-induced pyroptosis upon *S. typhimurium* infection of human epithelial cells.

A-D. LDH release in VPS4A$^{WT/E228Q}$ or CHMP3$^{WT/1-179}$ HeLa cells stably transduced with HA-tagged Dox-inducible VPS4A or CHMP3 constructs (CHMP3^{WT}, CHMP3$^{1-179}$, VPS4a^{WT} or VPS4a^{E228Q}) after infection with different MOIs of Δ*sifA S. typhimurium*. Protein expression was induced using 1.0 μg/ml Dox for 12 hours and then cells were infected for 5 hours (**A-B**) or for the indicated time-points (**C-D**). **E-F.** HeLa cells stably transduced with HA-tagged Dox-inducible VPS4A or CHMP3 constructs were seeded onto 96-well plates and infected with Δ*sifA S. typhimurium* for 2 hours, in order to determine bacterial invasion. The levels of intracellular bacteria were assessed by gentamicin

protection assay and CFU counting after plating onto LB agar plates. In **C-D**, the MOI was lowered in order to have no pyroptotic cell death at early time-points upon bacterial invasion, which would negatively impair intracellular bacterial survival, as observed with MOIs > 50 (data not shown). Graphs shown in **C-F** correspond to the same experiment. Graphs show mean ± SD. **P*<0.05; ***P*<0.01; ****P*<0.001; *****P*<0.0001; ns, not significant; student's t-test. Results are representative of at least three independent experiments performed in triplicate.

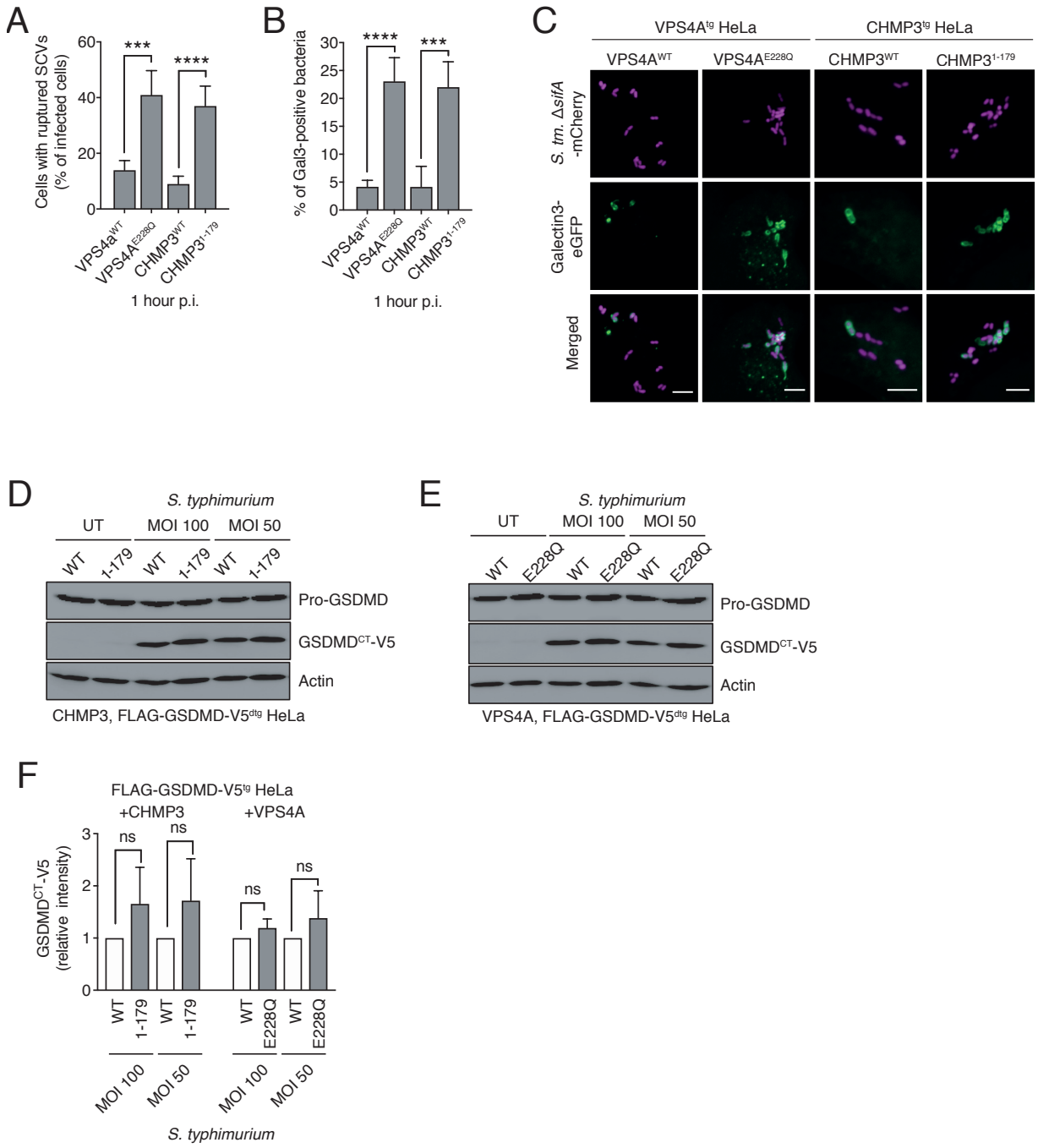

Fig. S15. ESCRTs regulate membrane integrity of the *Salmonella*-containing vacuole (SCV).

A-C. HeLa cells stably transduced with HA-tagged Dox-inducible VPS4A or CHMP3 constructs (CHMP3^{WT}, CHMP3$^{1-179}$, VPS4a^{WT} or VPS4a^{E228Q}) were transfected with a plasmid encoding galectin3-eGFP. Cells were then infected with Δ*sifA S. typhimurium*-expressing mCherry for 1 hour, fixed and imaged by confocal microscopy. Galectin3 accumulation can be used as a marker of lysed vacuoles, thus SCV rupture was quantified by assessing the

presence of intracellular bacteria positive for galectin3-eGFP. The percentage of infected cells containing galectin3-positive *S. typhimurium* (**A**) or the percentage of intracellular bacteria positive for galectin3 (**B**) was quantified by counting at least 50 infected cells or 200 bacteria per coverslip, respectively. Representative fluorescence confocal microscopy images (**C**) show the accumulation of galectin3-eGFP (green) around intracellular bacteria (magenta). Images were acquired using a 63x/1.40-NA oil objective and data were analyzed using FiJi software. All derived images shown correspond to 3D maximum projections and scale bars correspond to 5 µm. **D-E.** GSDMD processing 5 hours after infection with different MOIs of Δ*sifA S. typhimurium* in HeLa cells stably transduced with FLAG-GSDMD-V5 and HA-tagged Dox-inducible VPS4A or CHMP3 constructs. GSDMD processing was analyzed in combined lysate and supernatants by immunoblotting. **F.** Densitometric quantification (as described in Material and Methods) of GSDMD processing from HeLa cells stably transduced with HA-tagged Dox-inducible VPS4A or CHMP3 constructs 5 hours after infection with different MOIs of Δ*sifA S. typhimurium.* In all experiments protein expression was induced using 1.0 µg/ml Dox for 12 hours. Graphs show mean ± SD. ***$P<0.001$; ****$P<0.0001$; ns, not significant; student's t-test. Results are either pooled from two independent experiments performed in triplicate (**A-B**) or representative from two (**C**) or three (**D-F**) independent experiments.

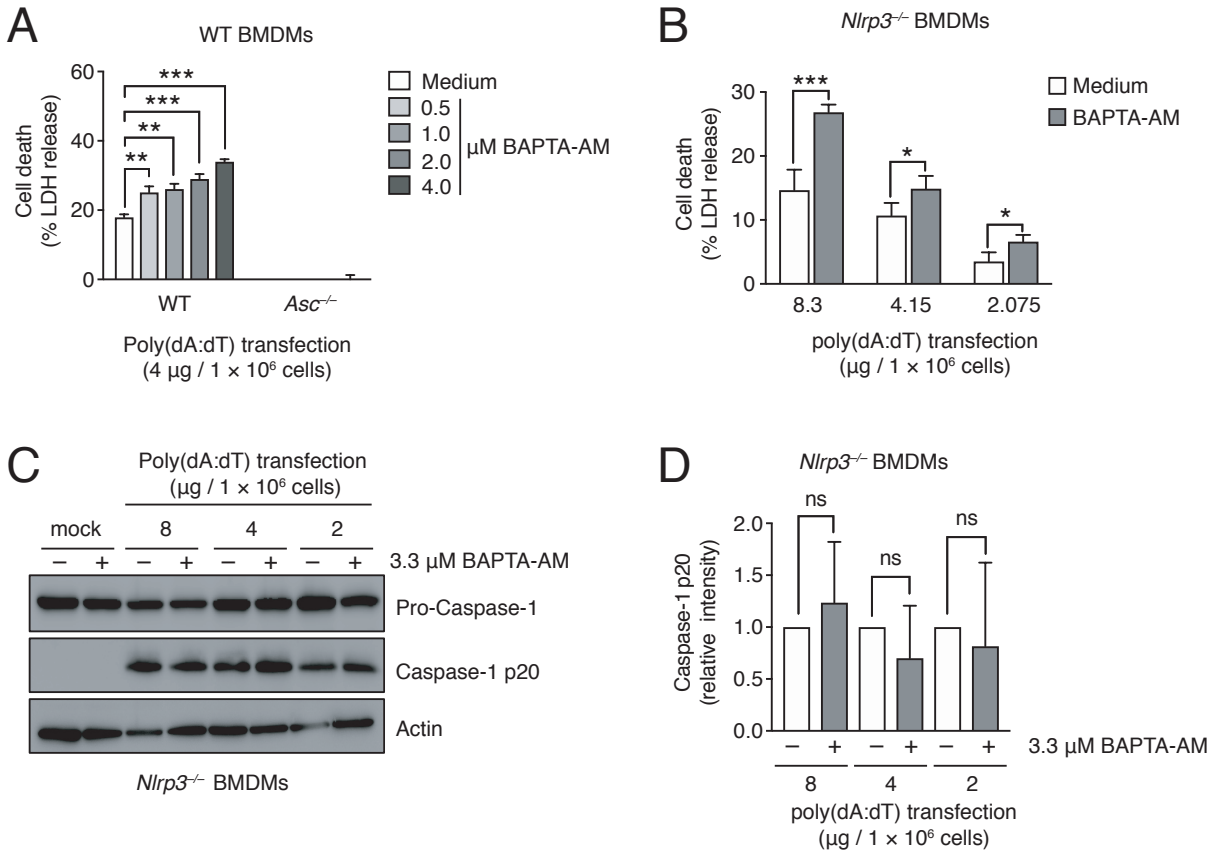

Fig. S16. Calcium chelation enhances cell death but not caspase-1 processing after AIM2 activation.

A-C. LDH release and caspase-1 processing in untreated or BAPTA-AM-treated *Nlrp3*$^{-/-}$ BMDMs transfected with poly(dA:dT) for 2 hours. **D.** Densitometric quantification (as described in Material and Methods) of the processed caspase-1 p20 band in untreated or BAPTA-AM-treated *Nlrp3*$^{-/-}$ BMDMs 2 hours post poly(dA:dT) transfection. Results show combined data of n=3 repeats. Results are expressed as intensity relative to the caspase-1 p20 in untreated controls. A representative immunoblot is shown in Figure S16C. Graphs show mean ± SD. **P*<0.05; **P <0.01; ****P*<0.001; ns, not significant; student's t-test. Results are representative of at least three independent experiments. *Nlrp3*$^{-/-}$ BMDMs are used to avoid GSDMD-dependent activation of NLRP3 and subsequently enhanced caspase-1 processing.

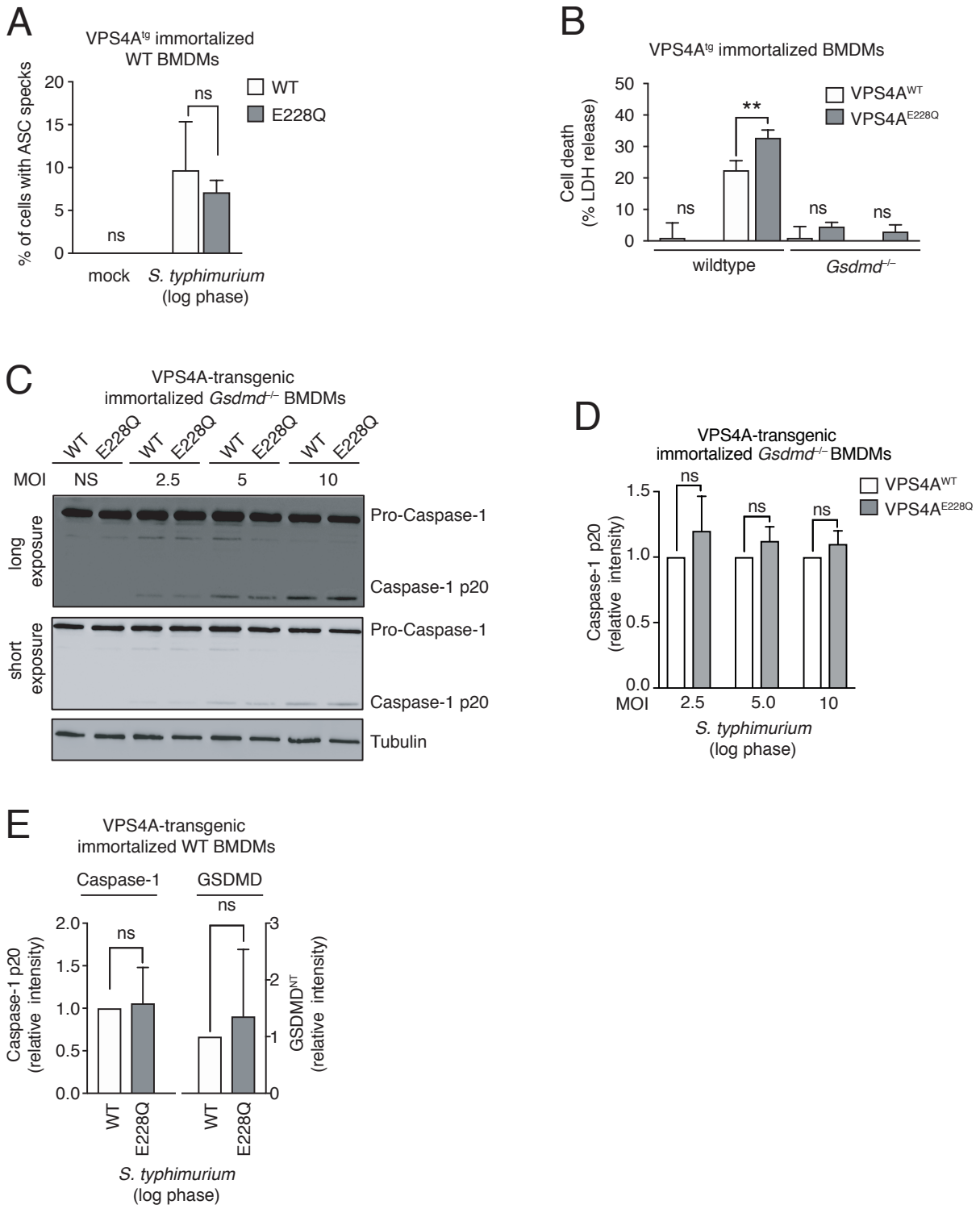

Fig. S17. ESCRT inhibition enhances pyroptosis after canonical inflammasome activation.

A. Percentage of cells with ASC specks in VPS4A^{WT}- or VPS4A^{E228Q}-transgenic wildtype iBMDMs after infection with log-phase *S. typhimurium* (MOI 10) for 1 hour. ASC specks were visualized by immunofluorescence and counted

as described in Material and Methods. **B.** LDH release from immortalized wild-type or *Gsdmd*$^{-/-}$ BMDMs stably transduced with indicated Dox-inducible VPS4A constructs after infection with *S. typhimurium* (MOI 5) for 1 hour. **C.** Immunoblot for caspase-1 processing in *Gsdmd*$^{-/-}$ iBMDMs stably transduced with indicated Dox-inducible VPS4A constructs after infection with log-phase *S. typhimurium* (MOI as indicated) for 1 hour. **D.** Densitometric quantification (as described in Material and Methods) of the processed caspase-1 p20 in VPS4A^{WT}- or VPS4A^{E228Q}-transgenic *Gsdmd*$^{-/-}$ iBMDMs infected with log-phase *S. typhimurium* for 1 hour. Results show combined data of n=3 repeats. Results are expressed as intensity relative to the processed protein in VPS4A^{WT}-expressing cells. A representative immunoblot is shown in Figure S18C. **E.** Densitometric quantification (as described in Material and Methods) of the processed caspase-1 p20 and GSDMD^{NT} bands in VPS4A^{WT}- or VPS4A^{E228Q}-transgenic wildtype iBMDMs infected with log-phase *S. typhimurium* for 1 hour. Results show combined data of n=3 repeats. Results are expressed as intensity relative to the processed protein in VPS4A^{WT}-expressing cells. A representative immunoblot is shown in Figure 4B. Graphs show mean ± SD. ** P <0.01; ns, not significant; student's t-test. Results are representative of at least three independent experiments. Protein expression in A-C was induced with 0.5 μg/ml Dox for 12 hours.

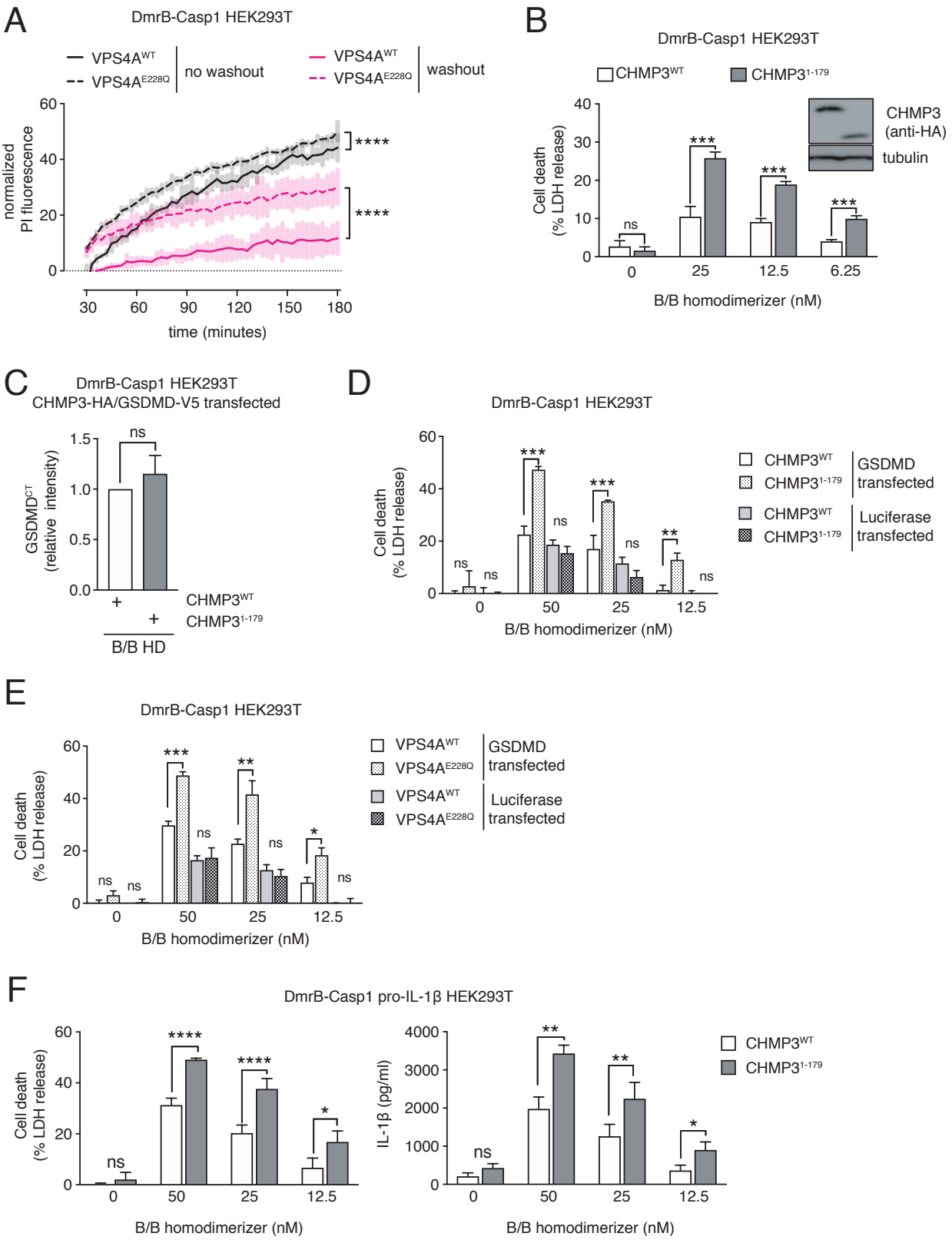
A
DmrB-Casp1 HEK293T
VPS4A^WT
VPS4A^E228Q
no washout
washout
normalized PI fluorescence
time (minutes)
****
B
DmrB-Casp1 HEK293T
CHMP3^WT
CHMP3^1-179
Cell death (% LDH release)
CHMP3 (anti-HA)
tubulin
B/B homodimerizer (nM)
C
DmrB-Casp1 HEK293T
CHMP3-HA/GSDMD-V5 transfected
GSDMD^CT (relative intensity)
B/B HD
D
DmrB-Casp1 HEK293T
GSDMD transfected
Luciferase transfected
E
DmrB-Casp1 HEK293T
F
DmrB-Casp1 pro-IL-1β HEK293T
IL-1β (pg/ml)

Fig. S18. ESCRT inhibition enhances cell death upon B/B homodimerizer-induced activation of DmrB-Casp-1. **A.** Time course of PI staining in DmrB-Casp1-transgenic HEK293T cells expressing FLAG-hGSDMD-V5 and Dox-inducible VPS4A constructs. Cells were treated with 25 nM B/B homodimerizer at t=0 and (optionally) 50-fold excess washout compound at t=30 minutes. **B.** LDH release at 120 minutes post treatment from DmrB-Casp1-transgenic HEK293T cells expressing Dox-inducible CHMP3 constructs treated as in A, except for varying B/B homodimerizer concentrations. Immunoblots show equal expression levels of CHMP3 proteins. **C.** Densitometric quantification (as described in Material and Methods) of the processed $GSDMD^{CT}$ band at 1 hour post treatment in DmrB-Casp1-transgenic HEK293T cells expressing FLAG-hGSDMD-V5 and Dox-inducible CHMP3 constructs. Cells were treated with 25 nM B/B homodimerizer at t=0 and 50-fold excess washout compound at t=30 minutes. Results show combined data of n=3 repeats. Results are expressed as intensity relative to the processed protein in $CHMP3^{WT}$-expressing cells. A representative immunoblot is shown in Figure 4E. **D-E.** LDH release from DmrB-Casp1-transgenic HEK293T cells expressing FLAG-hGSDMD-V5 or Luciferase, and Dox-inducible VPS4A/CHMP3 constructs. Cells were treated with 25 nM B/B homodimerizer at t=0 and 50-fold excess washout compound at t=30 minutes. **F.** LDH and IL-1β release at t=90 minutes from DmrB-Casp1- and pro-IL-1β-double transgenic HEK293T expressing FLAG-hGSDMD-V5 and Dox-inducible VPS4A constructs. Cells were treated with B/B HD at t=0 and 50-fold excess washout compound at t=30 minutes. Graphs show mean ± SD. **P*<0.05; ***P*<0.01; ****P*<0.001; *****P*<0.0001; ns, not significant; student's t-test. Results are representative of at least three independent experiments. Expression of WT or dominant-negative ESCRT proteins was induced for 16 hours (1 μg/ml doxycycline).

Movie Captions

Movie 1. Pam_3CSK_4-primed wildtype (left) and *Casp11*-deficient (right) BMDMs were loaded with 4 μM Fluo-8 (green) and subsequently transfected with LPS. Images were acquired in the presence of PI (red) every 30 seconds. Time is shown in minutes:seconds.

Movie 2. Pam_3CSK_4-primed wildtype (left) and *Gsdmd*-deficient (right) BMDMs were loaded with 4 μM Fluo-8 (green) and subsequently transfected with LPS. Images were acquired in the presence of PI (red) every 30 seconds. Time is shown in min:seconds

Movie 3. CHMP4-GFP HeLa cells stably transduced with Dox-inducible $GSDMD^{NT}$ were treated with doxycycline for 3 hours and subsequently imaged. Images were acquired every 10 seconds in the presence of PI (red). Time is shown in minutes:seconds.

Movie 4. Related to Figure 2B. Time-lapsed confocal images of either CHMP4-mCherry-expressing DmrB-Casp-1-transgenic HEK293T cells stained with Annexin-V as membrane marker. A cell expressing high level CHMP4 was chosen for imaging. B/B homodimerizer was added at t=0.

Movie 5. Related to Figure 2C. Time-lapsed confocal images of either CHMP4-GFP (in red)-expressing DmrB-Casp-1-transgenic HEK293T cells stained with Annexin-V as membrane marker. A cell expressing high level CHMP4 was chosen for imaging. B/B homodimerizer was added at t=0.

Movie 6. Related to Figure S5A. Time-lapsed confocal images of either CHMP4-mCherry-expressing DmrB-Casp-1-transgenic HEK293T cells stained with Annexin-V as membrane marker. A cell expressing high level CHMP4 was chosen for imaging. B/B homodimerizer was added at t=0.

Movie 7. Related to Figure S9. $VPS4A^{WT}$ (GFP-labeled)- and $VPS4A^{E228Q}$ (unlabeled) expressing immortalized WT macrophages were transfected with LPS and imaged in the presence of PI (red) every 5 minutes.

Movie 8. Related to Figure S9. VPS4A^{WT} (unlabeled)- and VPS4A^{E228Q} (GFP-labeled) expressing immortalized WT macrophages were transfected with LPS and imaged in the presence of PI (red) every 5 minutes.